Tutors

Dr. Rodrigo Soto López

Dr. Juan Llorens Llacuna
Departament of Chemical Engineering
and Analytical Chemistry

Grau en Enginyeria Química

Treball Final de Grau

Study of pervaporation in continuous regimen through aqueous solvent mixtures

Álex Santiago Negredo

June 2023

UNIVERSITAT DE BARCELONA

Lo que nos hace grandes es el hecho de poder ver lo pequeños que somos.

Carl Sagan

En primer lugar, me gustaría agradecer a mi tutor, el Dr. Rodrigo Soto, quien me ha enseñado que hacer ciencia puede ser de lo más emocionante y divertido. Por haberse implicado tanto en el proyecto, por haberme ayudado en todo lo que le ha sido posible y más, por haberme enseñado aspectos tan interesantes de esta profesión y a ser crítico con mi trabajo y sobre todo por el trato tan cercano que ha tenido conmigo. Sin él este trabajo no hubiese sido posible. También quiero agradecer al Dr. Juan Llorens Llacuna por la ayuda que ha estado dispuesto a proporcionarme en cualquier momento, aportando mucha riqueza y rigor al proyecto.

Darles las gracias también a las técnicas de laboratorio Olga y Belén, que han estado ayudándome día a día con cualquier problema que encontraba e incluso haciéndome reír cuando las cosas se torcían.

Por otro lado, agradecer a mis amigos y compañeros de carrera, sin los cuales a día de hoy no estaría donde me encuentro. Desde los momentos buenos, llenos de carcajadas, hasta los más duros: siempre han estado allí para apoyarme incondicionalmente.

Y por último dar las gracias a mi familia, que siempre me han ayudado y motivado para que sacase mi mejor versión. Su apoyo y confianza han sido cruciales en el transcurso de estos años.

CONTENTS

SUMMARY

Membrane processes are advanced filtration processes that allow component separation using membrane materials. The technique fundamentally separates a mixture of components physically, i.e. avoiding the need for additional chemicals to the feed stream to favour the separation. Nowadays, the industrial use of membranes is increasing due to their low energy demand, high separation efficiency, and their ability to maintain efficiency while reducing the number of steps, among other benefits.

Pervaporation (PV) is a membrane-based process that uses a permselective membrane to separate liquid mixtures using pressure gradient as the driving force. It presents potential application in situations where other separation processes are unfeasible (e.g. for separating mixtures of liquids with similar boiling points or azeotropic mixtures). In addition, it can be easily scaled-up and integrated with ease with other unit operation, making PV a versatile unit operation with realistic applicability in many areas. PV also plays a significant role in addressing the growing need to reduce the environmental impact of industrial activities, as it requires minimal energy consumption, and it does not generate waste products. Some important fields of application where pervaporation stands up by its effectiveness are separation of azeotropes, of substances with similar boiling points, of isomers, of heat-sensitive liquid mixtures, of volatile organic compounds (VOCs), and of trace contaminants in industrial effluents. Other industrial applications include the separation of organic liquid mixtures, organic substance extraction from aqueous mixtures and solvent dehydration.

This study focuses on evaluating the performance of PV in the separation of organic solvents, specifically acetone, from aqueous solutions, operating in continuous mode. The effect of different operating conditions such as feed flow rate and acetone concentration will be assessed. In addition, the effectiveness of the same polysiloxane (silicone) membrane for separating other pure organic solvents, e.g. methanol, ethanol, 1-butanol, methyl tert-butyl ether (MTBE), and a mixture with representative composition of the ABE (acetone, butanol and ethanol) fermentation process, has also been studied. The selectivity a d permeability of the membrane are found to depend on the molar flow, composition and chemical nature of the feed stream. Finally, a

subjacent objective underneath this work is to provide data for implementing a laboratory practice of pervaporation within the lab modules of the Chemical Engineering degree of the University of Barcelona.

Keywords: Membrane separation processes; silicone; pervaporation; organic solvents; acetone.

RESUMEN

Los procesos de membrana son aquellos procesos de filtración avanzados que permiten la separación de componentes mediante el uso de membranas de diferente naturaleza química. Estos procesos realizan una separación física de los componentes, siendo generalmente prescindible la adición de sustancias químicas en el alimento para favorecer la separación. Las operaciones con membranas se utilizan cada vez más en la industria debido a su baja demanda energética, su eficiencia de separación y su capacidad de mantener dicha eficiencia reduciendo el número de etapas, entre otros.

La pervaporación (PV) es un proceso de membrana que hace uso de una membrana selectiva para separar mezclas líquidas utilizando como fuerza impulsora el gradiente de presión que hay en la membrana. Presenta aplicabilidad en situaciones en las que otros procesos de separación no podrían llevarse a cabo, como para separar mezclas de líquidos con puntos de ebullición similares donde la destilación no es una opción o para separar mezclas de azeótropos. Su fácil escalabilidad y capacidad de integración junto a otras operaciones unitarias convierten a la pervaporación en una operación de separación de gran utilidad. Además, también tiene un papel importante en la actualidad con respecto a la incipiente necesidad de reducir el impacto ambiental producido por la actividad industrial ya que no requiere de grandes cantidades energéticas y no genera residuos. Entre las áreas de aplicación más importantes de la PV, demostrando mayor efectividad que otros procesos, destacan la separación de azeótropos, sustancias con puntos de ebullición muy similares, isómeros, mezclas de líquidos sensibles al calor, compuestos orgánicos volátiles (COVs) y trazas de contaminantes en efluentes industriales. Otras aplicaciones ampliamente extendidas en la industria son la separación de mezclas líquidas de orgánicos, la extracción de sustancias orgánicas de mezclas acuosas y la deshidratación de disolventes.

Este trabajo estudia el desempeño de la pervaporación en la separación de disolventes orgánicos de mezclas de acetona operando en continuo, en condiciones variables de caudal y

concentración de acetona en el alimento. El principal objetivo es evaluar la eficiencia del proceso en función de esas variables en el dispositivo experimental utilizado, el cual se ha sometido a mejoras progresivas. Además de mezclas acuosas de acetona, también se ha estudiado la pervaporación en la misma membrana (de silicona) de otros disolventes orgánicos puros de interés como metanol, etanol, 1-butanol, metil tert-butil éter (MTBE) y una mezcla representativa del proceso de fermentación ABE (acetona, butanol y etanol). Por último, un objetivo subyacente adicional es la utilización de la información adquirida para implementar nuevamente una práctica de pervaporación dentro de la oferta de prácticas de laboratorio que ofrece el Grado en Ingeniería Química de la Universidad de Barcelona.

Palabras clave: Procesos de membrana; silicona; pervaporación; disolventes orgánicos; acetona.

SUSTAINABLE DEVELOPMENT GOALS

In this work, pervaporation performance using a silicone membrane for the separation of acetone from aqueous mixtures operating in continuous mode is studied. Additionally, its efficiency for other pure solvents recovery and the separation of acetone from an ABE fermentation process blend and has also been assessed. PV is a unit operation that barely generates waste and does not require as much energy as other separation processes, being a very promising alternative regarding its low environmental impact.

As for sustainable development goals, pervaporation process in an industrial scale address 3 of the 5 Ps [1]: people, prosperity, planet and partnership.

- Prosperity: the process focuses on Industry, innovation and infrastructure (9). Pervaporation aims to improve separation efficiency in some applications, being more promising than other unit operations when determined conditions take place.
- Planet: Climate action (13), Life below water (14) and Life on land (15) are targeted in pervaporation. Concerning climate action, the process almost generates zero waste and requires low amounts of energy compared to other unit operations. As for life below water and life on land, one application area of pervaporation is the separation of pollutants from ground, surface and industrial water streams, improving its quality when returned to the environment.
- Partnership: Partnership for the goals (17) is addressed since pervaporation is a process that still has some limitations in many aspects, willing to be improved in the future.

1. INTRODUCTION

1.1. PERVAPORATION FUNDAMENTALS

Pervaporation is a separation technique used for liquid mixtures. It has gained considerable attention in recent years due to its efficiency and versatility. For instance, its applicability in situations where other processes could not be carried out, its easy scalability and its ability to integrate with other unit operations. Additionally, it also reduces the process' environmental impact as it does not require large amounts of energy and does not generate waste. This technique is based on the use of a selective membrane with a physicochemical nature that enables the selective separation of components in a mixture by selectively evaporating one or more of them and permeating their vapours through the membrane. It is worth noting that PV is the only membrane process in which there is a phase change from liquid to vapour and the driving force is the difference between the vapour pressure of the species to permeate and the partial pressure of this species in the permeate side.

1.1.1. Historical background

The origin of this process dates to the early 20th century, specifically in 1906, when Kahlenberg used a thin layer of rubber to separate hydrocarbons and alcohols [2]. However, it was Kober who coined the term when studying the selective permeation of water from albumin and toluene aqueous solutions through cellulose nitrate films [3]. It was upon observing this permselective evaporation that he decided to merge both concepts into "pervaporation". Later, in 1976, Aptel *et al*. introduced this operation in the separation of azeotropic mixtures [4]. However, it wasn't until Binning *et al*. applied the process for the separation of hydrocarbon mixtures through dense polyethylene films that it was systematically used. In this study, they observed that linear hydrocarbons permeated more rapidly than branched isomers [5]. Since then, the use of

pervaporation has been increasing, leading to significant advances in the underlying mass transport mechanisms through membranes and the synthesis of membranes with improved selective properties. For example, multiple organophilic and hydrophilic membranes were created for the dehydration of organic solvents (a process that gained momentum in the 2000s-2010s) and later for the purification of organic solvents.

1.1.2. Physicochemical principles

Pervaporation is based on the difference in the adsorption and diffusion properties of the components in a selective membrane. The driving force behind PV is the chemical potential gradient of the mixture, although the most determining aspect is the difference in partial pressure of the components on both sides of the membrane, as well as the molecular interactions between the components and the membrane [6]. This pressure gradient corresponds to the difference between the vapor pressure of the liquid and the partial pressure of the permeating species on the other side of the membrane (in the PV cell). To ensure that this gradient is enough for the liquid to permeate, a vacuum pump is used in the pervaporation cell to maintain the partial pressure close to zero. One way to increase this pressure difference is by increasing the feed temperature, so that the vapor pressures of the liquids are even higher. When this driving force is applied, substances with affinity to the membrane permeate in the form of vapor, and it is common to condense them again after its recovery.

It should be noted that in pervaporation, there is not only a mass transfer through the membrane but also a heat transfer. The change of state from liquid to vapor requires energy (vaporization enthalpy), which is extracted from the feed stream, decreasing thereby the temperature of the retained portion (the part of the mixture that did not permeate). This effect increases with higher liquid permeability since evaporation rate is faster. Therefore, in industrial-scale applications, a heat exchanger is usually added to the process to maintain a constant temperature [7].

There are two models that explain the mechanism of mass transfer: i) the solution-diffusion model [8] and, ii) the pore flow model [9]. The most commonly used is the solution-diffusion model

(Figure 1), which assumes the following aspects [7]: i) membrane as a homogeneous medium, ii) isothermal system, iii) steady state, iv) there is no convection but only diffusion and thus first law of Fick applies, v) no coupling mass transport effects, and vi) interphase equilibria.

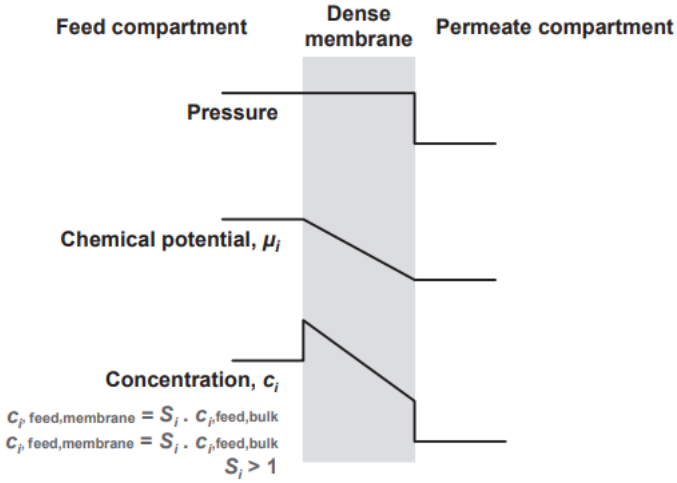

Figure 1. Mass transport through a pervaporation dense membrane according to the sorption-diffusion model (diagram from *Crespo et al*., ref [7])

The solution-diffusion model theorizes that solubility and diffusivity are the two determining factors in a process where a component *i* selectively sorbs through the membrane due to its higher affinity for the membrane compared to the feed mixture. This affinity is quantified by the sorption coefficient (S_i). As shown in Figure 1, there is a concentration gradient in the membrane, which causes the compound to diffuse to the surface of the permeate part of the membrane. This diffusion naturally depends on the diffusion coefficient D_i [m^2/s]. Finally, the permeating compound instantaneously desorbs at the permeate interface.

1.1.3. Performance evaluation parameters in pervaporation

There are several parameters useful for evaluating the pervaporation. The most relevant ones are flux (J_i), separation factor (β_{ij}), permeability (P_i), permeance (P_i/l) and selectivity (α_{ij}). Among

them, flux and separation factor are those used more often in PV studies. As discussed by Baker *et al.* [10] the use of fluxes and separation factors can lead to a difficult comparison of pervaporation data because these are not only a function of the intrinsic properties of the membranes used, but also depend on the operating conditions, which results in different values under different experimental conditions. Accordingly, expressing results in a normalized form as permeabilities, permeances and selectivities is adviced. In the present study, permeabilities (P_i) are used, as recommended by Baker *et al.*, but for separation efficiency, separation factors (β_{ij}) instead of selectivities (α_{ij}) will be used due to the requirements of the plug-flow model assumed (described later). This means that permeabilities will indeed be normalized values prone to be extrapolated to other experiments, but separation factors will only be valid under the specific process conditions explored.

Permeability (P_i) refers to the permeation rate of a substance penetrating another material, generally under specific conditions of temperature and pressure. Permeance (P_i/l) reflects the permeability by a specific membrane width (l). This means that while permeability is an intrinsic property of the membrane material, permeance is a specific membrane property. Based on these definitions, permeability has been chosen upon permeance to express the experimental results of this work with the aim of obtaining results suitable for comparison with other studies. Permeability (mol s^{-1} m^{-1} Pa^{-1}) of a pure substance can be expressed by Eq.1:

$$P_i(1) = \frac{J_i \cdot l}{\left(p_{i_o} - p_{i_l}\right)} \qquad \text{(Eq.1)}$$

where J_i is the permeate flux (mol m^{-2} h^{-1}), l is the membrane width (m), p_{i_o} is the vapour pressure (Pa) of the permeating component and p_{i_l} (Pa) is the partial pressure of the vapour in the permeate side.

Separation factor (β_{ij}) is the ratio of the molar component concentrations in the fluids on either side of the membrane. It quantifies how compound *i* is preferably permeated through a certain material when compared to the permeation of compound *j*. It can be determined in two different ways by either Eq. 2 or Eq. 3:

$$\beta_{ij} = \frac{P_i \cdot p_{i_o}}{P_j \cdot p_{j_o}} \quad \text{(Eq. 2)}$$

$$\beta_{ij} = \frac{{Y_i}/{Y_j}}{{X_i}/{X_j}} = \frac{{Y_i}/{(1-Y_i)}}{{X_i}/{(1-X_i)}} \quad \text{(Eq. 3)}$$

where *Y* is the molar fraction in the vapour phase (permeate side) and *X* is the molar fraction in the feed liquid phase.

As separation factor increases, membrane selectivity will also increase, meaning that separation will be easier. If β_{ij} surpasses de unit, the component of interest (component *i*) will preferentially permeate while if it remains under the unit, component *j* is the one that preferentially permeates. If it is equal to 1, there is no selective permeance and both components will permeate at the same rate.

1.2. FACTORS AFFECTING PERVAPORATION PERFORMANCE

Several factors influence the efficiency and separation factor of a pervaporation process, and their understanding and optimization is essential to achieve an efficient and cost-effective separation through PV. These factors include the feed flow rate, the partial pressure of the components, the composition of the feed mixture, the operating temperature, and membrane properties such as thickness and selectivity, among others. The material conforming the membrane is also crucial, as it will be later discussed.

1.2.1. Feed flow rate

Increasing the flow rate, and consequently the flux, leads to a better penetration of the molecules in the membrane, increasing its hydrophobic properties, then becoming more selective [11] and enhancing the separation factor. As observed by Jain *et al.* [12] when studying the pervaporation for ethanol-water separation using a commercial polydimethylsiloxane (PDMS) membrane, the separation factor increased from 3.1 to 4.2 when increasing feed flow rate from 50 to 100 L/h.

1.2.2. Permeate pressure

As aforementioned, permeate pressure is probably the most important aspect in PV performance, being the main driving force. As shown in Eq.1, the pressure gradient through the membrane has a huge effect on the permeability of a substance. The biggest gradient achievable corresponds the permeate with pressure equal to zero, which is virtually impossible to attain. Studying methanol pervaporation, Moulik et al. [13] observed that this driving force decreases at low vacuum, reducing the rate at which molecules desorb from the permeate interface. Therefore, both separation factor and permeation depend upon vacuum conditions.

1.2.3. Feed concentration

The effect of feed concentration is remarkable as well. Wilson *et al*. [14] studied the effect of feed composition of chloroform/acetone mixtures on the permeation rate and separation factor of poly(ethylene-co-vinyl acetate) nanocomposite membranes reinforced with cloisite 25 A°, where total flux increased with feed concentration. In the other hand, the membrane became less selective and consequently separation factor decreased. In other words, flux is directly proportional to feed concentration but separation factor is inversely proportional. However, permeability almost remains constant since the flux values are normalized as the driving force effect is removed [10]. It is interesting to say that, unlike vapour permeation, increasing pressure does not lead to a raise in concentration, due to the incompressibility of liquids.

1.2.4. Temperature

There are two reasons why temperature can affect pervaporation efficiency: because of the vapour pressure of the permeate liquid (the higher the feed temperature the higher the vapour pressure of the permeate substance, and thus higher pressure gradient) and through the thermal stimulation of the membrane polymer chains, causing a rise in permeation rate [15]. Both ways are translated into a rise in the permeate flux with temperature. This last reason can also be described by an Arrhenius-type relationship of the permeate flux [15]:

$$J = J_o \exp\left(-\frac{E_a}{R_g T} \right) \quad \text{(Eq. 4)}$$

where E_a is the activation energy (J/mol) associated with the permeate process, R_g is the gas constant (J mol^{-1} K^{-1}) and T is the feed temperature (K).

Apart from the mentioned effects, temperature has a negative effect on the separation factor, being inversely proportional to temperature [15]. This is a consequence of the free volume generated in the membrane when increasing the thermal motion, providing more space for molecular diffusion due to thermal expansion, hence decreasing selective permeation. In other words, flux does increase with temperature but selectivity decreases.

1.2.5. Membrane thickness

Membrane thickness also has an important role in pervaporation performance. In this case, the effect is inversely proportional since membrane resistances increase when increasing the thickness. Therefore, thin membranes offer less resistances, causing higher permeation fluxes [16]. As for the separation factor (β_{ij}), membrane thickness does not influence the separation characteristics of the polymer [6]. In conclusion, permeability decreases with the membrane width while separation factor does not depend on this factor.

1.3. MEMBRANES FOR PERVAPORATION

When selecting a membrane for a PV process, three aspects must be taken into account: selectivity, productivity and stability. There are different types of membranes used, and the main classification includes inorganic membranes, polymeric membranes and mixed matrix membranes (MMMs). Each type of membrane has its own characteristics and selectivity properties, making them suitable for different applications and/or operating conditions. The membrane choice also depends on whether we want to perform a hydrophilic, hydrophobic or organophilic pervaporation process. Choosing the right membrane is crucial to achieve the desired separation and maximize process efficiency. Nowadays, it is still a challenge finding membranes that offer high performance and long-term stability.

1.3.1. Inorganic membranes

The most frequently used inorganic membranes are composed of zeolites, silicas, titania and zirconia, generally used in pervaporation for separating of water from organic mixtures. Compared to polymeric membranes, the inorganic ones offer higher thermal and chemical stability, as well as greater selectivity [15]. However, they present some disadvantages, such as high fabrication cost, brittleness, complex preparation method and lack of technology to form defect-free and continuous membranes [15].

Figure 2. Inorganic membrane composed of zirconia (Made-in-China)

1.3.2. Polymeric membranes

This type of membranes may be the most widely used due to their high chemical stability, ease of being processed, excellent mechanical properties, thermal stability, etc. The main applications of these membranes are for dehydration of organic solvents, removal of organic components from water (as in this study), biofuels from fermentation broths, separation of organic mixtures and desulfurization of gasoline. Polymeric membranes can also be classified into natural and synthetic, both exhibiting excellent performance.

Among natural membranes, chitosan and sodium alginate are two well-known materials. The former is used for dehydration of organics and removal of alcohol from organics due to its hydrophilic nature [17]. The later, sodium alginate (NaAlg) is also a hydrophilic-type polymer used in the separation of water-organic mixtures [18], but not for commercial applications because of its pour selectivity and mechanical strength.

Synthetic polymers for PV membranes include polyether amides, polyurethanes, polymethyl methacrylates (PMMAs), polydimethylsiloxane (PDMS), polyacrylates, polyesters, polyethyleneimines, silicone composites (SC), and are used in many applications.

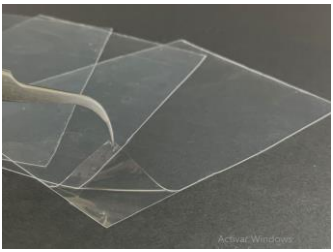

Figure 3. PDMS membranes (DiagnoCine)

1.3.3. Mixed matrix membranes (MMMs)

This type of membranes was designed mainly for combining properties of both inorganic and polymeric membranes, and their performance depend on the chosen inorganic fillers and solvent. For example, the porous magnesium oxide (MgO) particle-incorporated Matrimid matrix membranes showed higher selectivity in the dehydration of isopropyl alcohol [19]. Incorporating inorganic fillers such as zeolite, silica, MgO, etc. proved to offer very promising efficiency. Another interesting example of components with controllable pore sizes and high porosity would be metal-organic frameworks (MOFs), which present very high thermal and chemical stability [20].

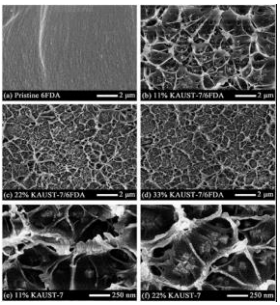

Figure 4. MMMs examples (image from ref. [21])

1.4. APPLICATIONS OF PERVAPORATION

1.4.1. Solvent dehydration

This application consists of the removal of water present in organic solvents using a hydrophilic membrane. It is widely employed specifically for the dehydration of alcohols such as ethanol, isopropanol, *tert*-butanol etc [6]. Alcohols have a strong affinity to water, easily creating an azeotropic mixture at a certain composition, being PV a very useful technique for their purification unlike distillation or solvent extraction.

1.4.2. Organophilic separation

This application has a very important role in environmental safety, e.g. recovering organic compounds from aqueous industrial streams. It is also used for alcohol isolation in bioethanol production, organic solvent recovery from gas scrubbing wash water and aroma recovery from plant extracts [6]. Despite being challenging areas of research, pervaporation allows to target all of them whilst still being economical. The membranes used are mostly hydrophobic and non-polar, resulting in less selective membranes since water molecules still manage to diffuse through the membrane due to their small size. Polydimethylsiloxane (PDMS) and polytrimethylsilyl-1-propyne (PTMSP) are the most used materials for hydrophobic membranes.

Among organophilic separation, two main applications can be distinguished [6]:

- Removal of VOCs: removing volatile organic compounds (VOCs) such as benzene, toluene, xylene, ethylbenzene… from surface water or ground water is one of the major applications of PV since conventional methods like distillation, adsorption and air stripping have some limitations (adsorbent regeneration, high energy consumption, and additional hazards caused by secondary pollutants). PDMS is one of the most popular membranes for VOCs removal due to its high selectivity and stability, but some other materials would be nitrile-butadiene copolymer (NBR), polyvinylidene fluoride (PVDF), styrene butadiene (SBS) and polyurethane (PUR).

- Extraction of aroma compounds: these include flavoured compounds from food, beverages and cosmetics, and some examples are acetaldehyde, 3-methyl butanal and some chemical species found in waxes, oils, coffee beans, pigments and dyes.

1.4.3. Organic/organic separation

This application includes the recovery of certain value-added organic compounds as well, from industrial process streams where other compounds that easily form azeotropic mixtures or have close boiling points are also present. The first applied evidences of this type of separation were in petroleum refineries for the recovery of toluene and styrene from various heavy, intermediate and light catalytic naphtha streams [22]. Moreover, pervaporation was also used for separating benzene from C_6 reformate stream used in the production of high-grade gasoline. Organic/organic separation by PV can in turn be classified into four subdivisions: i) separation of polar and non-polar solvents, ii) separation of aromatic and alicyclic mixtures, iii) separation of aromatic/aliphatic hydrocarbons, and iv) separation of isomers.

1.5. ADVANTAGES AND DISADVANTAGES OF PERVAPORATION

The main advantages of pervaporation can be summarized as follows [15, 23]:

- Azeotropes can be easily separated avoiding the need for additional substances.
- Solvents with similar volatility can be separated.
- Unlike solvent recovery using activated carbon adsorption, PV does not heavily dilute the recovered solvents with water. For instance, compared to distillation, it can save up to 35% of the energy consumed [24].
- It is more energy and cost efficient than conventional separation technologies [25], presenting also a lower environmental impact.
- Compared to other techniques, pervaporation does not require large operating space and is easily transportable, with remarkable operating simplicity.
- Ease of adaptability with other unit operations maintaining efficiency.
- Process is completely enclosed, minimizing direct and scape emissions.

Nonetheless, some limitations worth to mentioning exist. For instance, it requires purified feed and a temperature reduction affects detrimentally the transmembrane flux.

1.6. ABE FERMENTATION PROCESS

Acetone-butanol-ethanol (ABE) fermentation, also known as Weizmann process, is a process that uses bacterial fermentation to produce acetone, n-butanol and ethanol from carbohydrates such as starch and glucose. It was developed by Chaim Weizmann, and its primary use was for the production of acetone, needed to make cordite (essential in the British war industry during World War I). Nowadays, although it has proven to be a good option for industrial-scale production of biobutanol, the continuous fermentation process suffers from low product yield and productivity [26].

Organisms carrying out the fermentation must be anaerobic, and the bacteria used are usually from the class Clostridia (family Clostridiaceae). More specifically, the most well-studied one is *Clostridium acetobutylicum.* The fermentation process takes place in two phases: in the acidogenesis phase (second stage in the anaerobic digestion, where simple monomers are converted into volatile fatty acids) cells grow exponentially and accumulate acetate and butyrate. The second phase, solventogenesis (chemical production of solvents), starts with the low pH along with other factors given in the first stage. In this stage acetate and butyrate are used to produce solvents. These solvents are acetone, butanol and ethanol, usually produced in the proportions of 30%, 60% and 10%, respectively. Pervaporation plays a very important role in the separation of these solvents once the fermentation process has finished for their use in other processes.

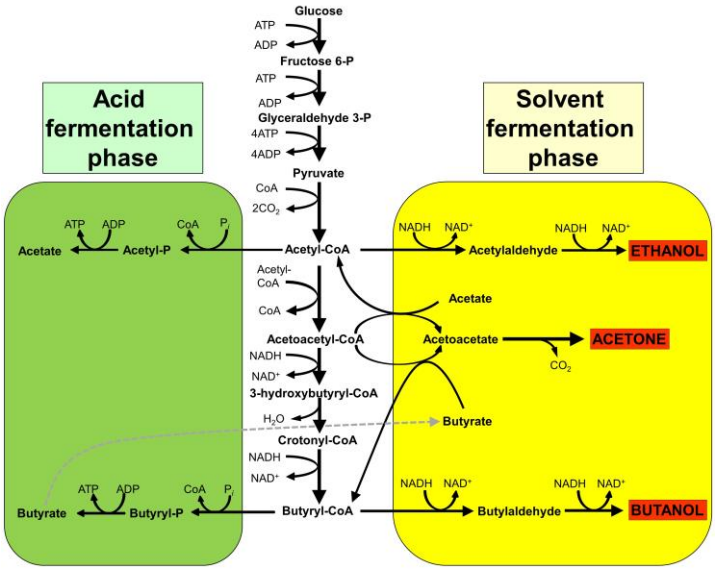

Figure 5. Phases of the ABE fermentation process

(Emply shell China dry, 2/10/2015 via Wikimedia Commons, Creative Commons Attribution)

2. OBJECTIVES

The main aim of this work is to study the performance of a continuous pervaporation process for the separation of acetone from aqueous mixtures using a silicone membrane. Accordingly, this system will be studied in more detail but other comparative approaches will also be evaluated aiming to increase our understanding about the behaviour of focused membrane under different situations. More specifically, the following subobjectives are established:

- To adapt the experimental setup in order to maximize the amount of permeate that can be recovered from the pervaporation process studied for the separation of acetone/water mixtures.
- To study the performance of a silicone composite (SC) membrane-type for separating acetone-water mixtures under different experimental conditions.
- To assess different ways for determining the composition of the permeate and retained parts of the membrane, including refractometry, UV-vis absorption and gas chromatography.
- To study the effect of composition and feed flow rate on the permeability (P_i) and acetone separation factor (β_{ij}) of the membrane/feed system studied.
- To study the permeability of other pure organic solvents such as methanol, ethanol, butanol and MTBE and to compare the results to those of pure acetone under identical feed flow rate to assess the potential of the studied membrane for other applications.
- To study qualitatively the potential of the setup studied for separating a mixture of acetone, butanol and ethanol with a composition representative of the ABE fermentation process, assessing thereby the applicability of PV and the studied membrane.
- To establish a reproducible experimental procedure of utility for further developing a possible Chemical Engineering degree lab practice.

3. EXPERIMENTAL SECTION

3.1. ORGANIC SOLVENTS USED

This study mainly focuses on the performance of pervaporation for acetone separation from binary aqueous mixtures. However, the permeability of other pure organic solvents has also been evaluated to assess the potential of this type of membrane for other applications. These are namely: methanol, ethanol, 1-butanol and methyl tert-butyl ether (MTBE). In addition, and given the prospective potential of PV to be coupled with the ABE (acetone-butanol-ethanol) fermentation process, a mixture with representative composition of the ABE output stream has been tested in the experimental setup to obtain some qualitative information regarding the capability of the technique. A brief description of the solvents used is provided below:

a) Acetone

Acetone (ACE), or dimethyl ketone, 2-propanone or beta-ketopropane (C_3H_6O, Figure 6), is a flammable and irritant manufactured chemical that is also found in low content in nature (in trees, plants, volcanic gases, forest fires and in the breakdown of bodyfat). It is also present in vehicle exhaust, tobacco smoke and landfill sites. ACE is used in many areas, e.g. for manufacturing plastics, fibers, drugs or other chemicals. It is also widely used to dissolve other substances, such as paints, and as nail polish removers. It has a role as a polar aprotic solvent provided by the carbonyl group, a human metabolite and an EC 3.5.1.4 (amidase) inhibitor. ACE is a colourless liquid, soluble in water, with a distinct sweetish smell, a density of 784 kg/m^3, and a flash point of -17.78 ºC. It evaporates easily with a normal boiling point of 56 ºC but molecules may start evaporating above -18 ºC.

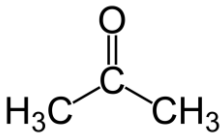

Figure 6. Acetone molecule

b) Methanol

Methanol (MeOH) or methyl alcohol (CH_3OH, Figure 7) is the simplest aliphatic alcohol, and also a methoxide conjugated acid. It is a flammable, acute toxic and health hazardous substance used to make chemicals, to remove water from automotive and aviation fuels, as a solvent for paints and plastics and as an ingredient in wide variety of products. It also has a role as an amphiprotic solvent, a fuel, a human metabolite, an Escherichia coli metabolite, a mouse metabolite and a Mycoplasma genitalium metabolite. MeOH is a colourless liquid with a sweet pungent odour, fully miscible with water with a density of 792 kg/m^3. It is quite volatile (boiling point is at 64.6 ºC) with a flash point at 11.11 ºC, being its vapours slightly heavier than air.

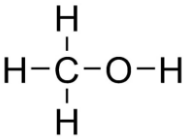

Figure 7. Methanol molecule

c) Ethanol

Ethanol (EtOH) or ethyl alcohol (C_2H_6O, Figure 8) is a colourless liquid with a very characteristic smell, fully miscible with water and a conjugated acid of an ethoxide. It is a flammable substance a role as an antiseptic drug, a polar solvent, a neurotoxin, a central nervous system depressant, a teratogenic agent, a NMDS receptor antagonist, a protein kinase C agonist, a disinfectant, a human metabolite, a Saccharomyces cerevisiae metabolite, an Escherichia coli metabolite and a mouse metabolite. It has a density of 789 kg/m^3, boiling point of 78.5 ºC and a

flash point at 12.78 ºC, being its vapours heavier than air. Under ambient conditions it is miscible in water at all concentrations.

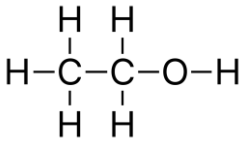

Figure 8. Ethanol molecule

d) 1-Butanol

1-Butanol (BuOH), n-butanol, butan-1-ol or butyl alcohol ($C_4H_{10}O$, Figure 9), is a colourless liquid, flammable, corrosive and irritant substance, of limited miscibility in water but is easily soluble in regular solvents such as ethers, alcohols, glycols and hydrocarbons. It has a density of 810 kg/m^3, a boiling point of 117.7 ºC and a flash point at 37 ºC. It is mainly used in organic chemical synthesis, plasticizers, detergents, etc. It also has a role as a protic solvent, a human metabolite and a mouse metabolite. It can be found in nature in humans (produced by the gut microbes), Vitis rotundifolia, Cichorium endivia and other organisms.

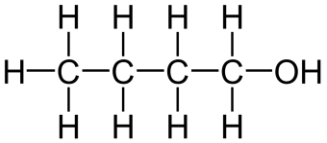

Figure 9. 1-Butanol molecule

e) Methyl *tert*-butyl ether (MTBE)

Methyl tert-butyl ether (MTBE, $(CH_3)_3COCH_3$, Figure 10) is a colourless liquid miscible with water with a distinctive, anaesthetic-like odour, a flammable and irritant liquid, synthesised form isobutylene and methanol that has been used as an additive for unleaded gasolines additive to increase octane rating and oxygen content. It has a density of 740 kg/m^3, a boiling point of 55 ºC and a flash point of -7.78 ºC, being its vapours heavier than air. It is used in medical treatments

to dissolve gallstones and in small amounts as a laboratory solvent. MTBE is almost completely banned in many US states due to concerns for groundwater contamination and water quality.

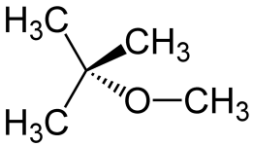

Figure 10. Methyl *tert*-butyl ether (MTBE) molecule

f) ABE (acetone-butanol-ethanol) fermentation process representative mixture

ABE refers to a chemical blend of acetone, butanol and ethanol obtained by fermentation using the Clostridium acetobutylicum bacteria currently used to produce biobutanol, among others. This process was introduced at industrial level in the 1920s, but until 1973, due to the oil crisis, it was not considered for BuOH production. Despite this promising application, ABE fermentation still suffers from drawbacks derived from the low yield and high energy requirement and by the fact that the bacteria used are inhibited by the butanol produced [27].

Typical yields from the ABE process are 30% ACE, 60% BuOH and 10% EtOH, but other process configurations may render 90% BuOH and 10% ACE and EtOH [28], all in w/w percentages.

3.2. EXPERIMENTAL SET UP

3.2.1. Final configuration

The final experimental set up, being the one that has been used in all the experiments, is composed of the following equipment:

- Two graduated test tubes of 100 mL used to contain the feed and the retentate. Must be made of glass to prevent solvent degradation and should be covered to avoid solvent evaporation.

- A peristaltic pump that allows mixtures and pure solvents flow through the system. More specifically, the Gilson Miniplus 3 peristaltic pump has been used, which can be configurated from 0 to 48 rpm.
- A cylindrical methacrylate pervaporation cell with a length of approximately 1 m and a diameter of 8 cm. The membrane is placed inside the cell, where vacuum is be applied, so it must be perfectly sealed, having only three orifices: one through which the load is fed, another through which the retentate is recovered and a last one through which the vacuum is applied and therefore the permeate recovered.
- A silicone tube that is used as pervaporation membrane. It has a length of 51.360 m, an internal diameter of 1 mm and an external diameter of 3 mm. Two additional tube segments (lengths are not important) connect the feed test tube with one of the PV cell orifices, passing through the peristaltic pump, and another orifice with the retentate test tube. An image of the transversal section of the tube is shown in Figure 11.
- A vacuum pump that applies vacuum in the pervaporation cell. The one used reaches vacuum pressures of 70-180 mbar.
- A vacuum meter to measure the vacuum pressure applied in the PV cell.
- A condenser for the recovery in liquid form of the permeate. The condenser is covered with glass wool in order to maximise thermal isolation. A round bottom flask is attached to the bottom end of the condenser to contain the condensed permeate.
- A chiller that refrigerates the condenser, reaching temperatures of up to -30 ºC. The coolant used is ethylene glycol 30%, having a freezing point of -18 ºC.
- A glass jar filled with water that is placed in the chiller's refrigerant tank in order to cool it down as much as possible. Connected to the top end of the condenser, a silicone tube of greater diameter with a 0.5 micron diffuser attached to its end is submerged in the jar in order to diffuse and dissolve in the water the acetone vapours that could not be condensed. The jar must be completely closed to avoid acetone vapour leaks, although an orifice should be made in the cap to prevent overpressure. It should be noted that acetone is being mixed with the liquid from which is being separated, but it is done only to quantify how much acetone is recovered.

- A scale to weigh all the containers and acetone mixtures and pure solvent loads. It has a precision of 0.01 g.

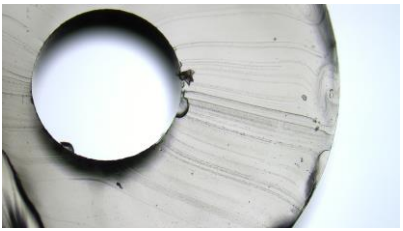

Figure 11. Optical microscopy image of the transversal section of the silicone membrane used

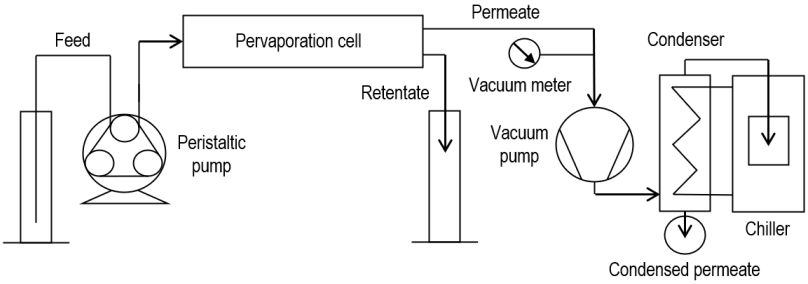

Figure 12. Experimental set up flow sheet

3.2.2. Progressive improvements of the experimental set up

In order to configurate the experimental set up that maximizes the amount of recovered permeate and more specifically the condensed fraction, many modifications have been made. The time invested in the search for the best configuration has been a lot. At first, no acetone was condensed. At first, a Torricelli was being used to measure vacuum pressure, so it was replaced with an electronic vacuum meter so the measures are more accurate. The second improvement was to incorporate the tube with the diffuser that connects the condenser with a jar full of water, since most of acetone vapours were escaping through the top orifice of the condenser. In this way, although there were still some leaks, part of the acetone vapours dissolved in water. The diffuser was added in order to produce smaller and easier to dissolve bubbles. This improvement allows to recover more acetone, but the main target is to increase the amount that is condensed.

In third place, the chiller was incorporated. This chiller could only reach a minimum temperature of -10 ºC. However, no condensed permeate was obtained yet. Next, the water in the jar was replaced by acetone and the jar was placed in a bucket with ice and salt in order to reduce even more the temperature. This would eliminate the problem of mixing with water the acetone recovered. Additionally, the chiller was placed in a higher place (reducing part of the potential energy required) and the connection tubes were cut in order to improve the refrigerant's flow and consequently decrease the temperature. It was observed that part of the jar's acetone evaporated, so it was replaced by water once again. In the other hand, condensed permeate was finally obtained, but still were some improvements that could be done in order to increase its amount. The next improvement was to cover the condenser with glass wool in order to increase thermal isolation. Moreover, water was once again replaced by acetone but this time using a volumetric flask (there is less evaporation surface), and it was introduced in the chiller's refrigerant tank to reduce even more its temperature. There still was evaporation. The last attempt on using acetone was performed with a flask filled with sand and acetone. The sand would act as a diffuser, increasing acetone recovery. Evaporation still took place, so using acetone to dissolve the permeate vapours was finally discarded despite the inconveniences of using water. However, using the chiller's refrigerant tank to reduce temperature was maintained. The last improvement that was done is to acquire a more powerful chiller, which reaches temperatures of -30 ºC (although such temperatures could not be used since water would freeze very quickly). With it, more acetone is successfully condensed.

3.3. EXPERIMENTAL PROCEDURE

3.3.1. Process preparation

In the first place, all the feed, retentate and permeate containers must be weighed in order to differentiate the amount of substance poured. These are the two glass test tubes, the condenser round bottom flask and the glass jar that is placed in the chiller's refrigerant tank. Secondly, the tube dimensions have to be measured. The silicone tube used in this study has a length of 51.360 m, an internal diameter of 3 mm and an external diameter of 1 mm. After, the tube has to

be placed once again in the PV cell, making sure it has been perfectly sealed to prevent leaks. In second place, a considerable amount of water must be made to flow through the system at the maximum pump configuration in order to clean the tube of possible dirt. When water is used, no refrigeration is needed since there should be no permeate. Using water as well, feed and retentate flow have to be calibrated. From this point, vacuum has to be activated. This calibration is done at 20, 30, 40 and 48 rpm since all the experiments will be performed at this pump configurations. Both the water fed and the one retained are poured in the test tubes, measuring the time it takes to feed/recover a certain amount of water in order to determine their flow rates. This calibration is done to ensure that the retained water is the same as the fed one given that there should be no permeate despite the vacuum is activated. Also, it will allow to know approximately which flow rates should be expected in the experiments. The last step prior to the experiments is to prepare the acetone-water mixtures. Six acetone compositions have been chosen, all in w/w: 0.90, 0.75, 0.50, 0.10, 0.05 and 0.01. The last three concentrations are so small because PV is often used for the removing of acetone traces in small concentrations from wastewater streams. The mixtures are made by adding gradually acetone and water in a glass jar that is being weighed. The jars must remain perfectly closed so acetone does not evaporate.

3.3.2. Experiment execution

The peristaltic pump used in all the experiments can be configurated from 0 to 48 rpm. Acetone-water experiments will be done, as it has already been said, at four different configurations for all the compositions: 20, 30, 40 and 48 rpm. However, as it will be discussed later, feed flow may vary from one composition to another, or even form one replicate to another. All experiments have been performed at ambient temperature, which goes from 19 to 26 ºC.

The first thing to do is to turn on the chiller in advance, as it lasts approximately 45 minutes to reach the set temperature. This temperature has to be low enough to maximize acetone condensation (refrigerant's freezing point has to be taken into account as well) but at the same time it has to be high enough so the water in the glass jar does not freeze instantly. The set temperature chosen for all experiments is -12 ºC. In second place, the external retentate tube has

to be put inside the retentate test tube and the glass jar filled with water in the chiller's refrigerant tank. The tube with the diffuser coming out of the condenser must be completely submerged in the jar, which has to be perfectly closed to prevent acetone vapour leaks. However, although some vapours will leak, a couple of orifices should be made to avoid overpressure in the jar.

Next, 100 mL of the mixture are poured into the feed test tube. It has to be weighed in order to know exactly how many grams of mixture are being fed. Both the retentate and feed test tubes should be covered to prevent acetone evaporation. Then, the external feed tube is placed inside the test tube, making sure its end touches the bottom to ensure all the load will be fed. Next, the vacuum pump is turned on and afterwards the peristaltic pump (at one of the chosen configurations), initiating the experiment. The silicone tube in the test tube increases a bit the load volume, so the chronometer has to be activated once it reaches 100 mL. From this point, time measures are taken every 10 mL in order to determine its associated feed rate. An additional timer should be started when the first retentate drop falls. It is recommended to take time measures every 10 mL when feeding low composition mixtures (X_m= 0.10, 0.05 and 0.01) and every 5 mL for high composition mixtures (X_m= 0.90, 0,75 and 0.50) since less solution will be retained. Values taken after the feed load is completely fed are no longer important since this work addresses pervaporation performance in continuous mode only. At this point, the peristaltic pump can be configurated at 48 rpm (if it was not already) in order to reduce the operating time. Another reason is because since no feed is left, the system is being fed with air, which is a compressible fluid. Therefore, part of the pumping power is destined to compress this air instead of pushing the liquid. At 48 rpm, the peristaltic pump still has enough power to push it till the end of the silicone tube.

During all the experiment, every certain amount of time, vacuum pressure has to be checked to make sure it does not vary drastically, and the tub with the diffuser should be moved so it does not get stuck in the frozen water. The experiment ends once the last retentate drop falls. Finally, the two test tubes, the jar filled with water and the condenser round bottom flask must be weighed, but previously making sure, as much as possible, the jar is not wet (otherwise the weight measure would not be precise) and that there are no permeate droplets yet to fall in the condenser. This

procedure has been repeated 3 times for every pump configuration and mixture composition, performing a total of 72 experiments.

As for pure solvent and the ABE blend experiments, the procedure is the same. Pure acetone experiments have to be done two times for all pump configurations (48 rpm configuration has been repeated a third time) whereas MeOH, EtOH, BuOH, MTBE and ABE blend experiments are only performed two times each at 48 rpm. The preparation of the ABE mixture is done by pouring acetone, 1-butanol and ethanol in the previously mentioned proportions in a glass jar. This has to remain completely closed to prevent compound evaporation.

3.3.3. Sample analysis

For sample analysis, three techniques were considered in the first place: refractometry, UV-vis absorption and gas chromatography. A calibration with multiple known-composition samples was made for each technique, but the first two methods were not considered feasible for the following reasons: refractometry, despite being easy to use, presented a parabola instead of a line, representing a problem because two composition values could be associated to a single refraction index.

In the other hand, for the UV-vis absorber's calibration, 1/200 dilutions had to be made for every known-composition sample since the absorber got saturated with such high acetone compositions, obtaining the same absorbance value in all of them. This was considered a problem because making 1/200 dilutions for every sample would have significantly slowed down the sample analysis process.

Gas chromatography does not present any apparent problem (the calibration of the chromatograph is shown in Figure A3), enabling the proper identification and quantification of the composition of permeate and retained streams and hence it has been chosen as the technique for sample analysis. 0.2 µL of the sample to be analysed were taken with a micro syringe (which must be washed before every sample) in all the analyses and injected to the GC. This integration of the chromatograms quantified as area were related to different compositions by a preliminary calibration using standards of different acetone-water known compositions.

3.4. CALCULATIONS

All equations require mol as mass unit so, in order to fit in the equations, experimental lectures of, for example, q (mL/s) and X_f (kg/kg) have been converted into mol/s and mol/mol, respectively.

Prior to the calculations, the silicone tube surface must be determined. Since the inner surface differs from the external surface, a logarithmic mean diameter (D_{ml}) has been calculated with the following expression:

$$D_{ml} = \frac{D_2 - D_1}{\ln\left(\frac{D_2}{D_1}\right)} \quad \text{(Eq. 5)}$$

where D_2 is the external diameter of the tube (m) and D_1 the inside diameter (m).

With D_2= 3 mm and D_1= 1mm, D_{ml} has a value of 1.82 mm and, therefore, knowing the tube has a length of 51.360 m, the permeating surface is 0.294 m^2.

3.4.1. Pure solvent permeabilities

To determine the permeabilities of pure substances such as acetone, methanol, ethanol, 1-butanol and MTBE, Eq 1 has to be used. Permeate flux (mol/(s·m^2)) is calculated with the following expression:

$$J_i = \frac{q_f - q_r}{S} = \frac{q_p}{S} \quad \text{(Eq. 6)}$$

where q_f is the feed flow (mol/s), q_r the retentate flow (mol/s), q_p the permeate flow (mol/s) and S the total permeating surface (m^2).

Since feed and retentate flows are determined experimentally and the permeating surface has already been calculated, flux can be known. Together with vapour pressures (easily found knowing the operating temperature), vacuum pressures (read on the vacuum meter) and the membrane thickness, which is 1 mm, permeabilities can be calculated. Since acetone experiments have been done at four different pump configurations, P_i has been calculated for all of them.

3.4.2. Acetone-water mixtures

Both P_i and β_{ij} can be calculated following too different models: mixed flow model and plug flow model. In order to determine which of these two models suit this study, Reynolds number has been considered:

$$Re = \frac{v \cdot D_1 \cdot \rho}{\mu} \quad \text{(Eq. 7)}$$

where v is the fluid speed inside de tube (m/s), ρ the mixture's density (kg/m^3) and μ the mixture's viscosity (kg/(m · s)).

The highest value of Re is 252.8, obtained at 48 rpm and X_m= 0.90. This clearly indicates that the fluid in all the experiments flow in a laminar way so, regarding as well that the tube has such a big length, the plug flow model has been considered as the one that suits best in this study.

Plug flow model considers that the fluid properties change longitudinally but remain constant radially, decreasing both q and X as the liquid flows through the tube since part of it is permeating through the membrane.

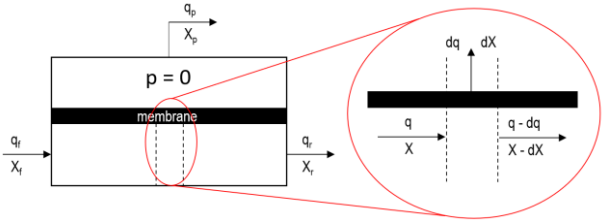

Figure 13. Plug flow model representation

For the calculation of the permeability of a substance in a binary liquid mixture of *i* and *j* components and its separation factor for a plug flow model, mass balances must be taken into account:

$$\text{Component } i\text{: } d(q \cdot X) = -(dS) \cdot P_i \cdot \frac{X \cdot p_{i_o}}{l} \quad \text{(Eq. 8)}$$

$$\text{Component } j\text{: } d\big(q \cdot (1 - X)\big) = -(dS) \cdot P_j \cdot \frac{(1-X) \cdot p_{j_o}}{l} \quad \text{(Eq. 9)}$$

where *q* is de molar flow (mol/s).

The global mass balance can be reorganized in order to obtain an expression for the calculation of permeate molar fraction (Y_p):

$$Y_p = \frac{1}{\theta}\left(X_f - (1-\theta)\cdot X_r\right) \quad \text{(Eq. 10)}$$

where θ is the product recovery fraction, X_f the molar fraction in the feed stream and X_r the molar fraction in the retentate stream.

Product recovery fraction is calculated with the following expression:

$$\theta = \frac{q_f - q_r}{q_f} = \frac{q_p}{q_f} \quad \text{(Eq. 11)}$$

Additionally, there are three dimensionless groups that take part:

$$q' = \frac{q}{q_f} \quad \text{(Eq. 12)} \qquad S' = S \cdot \frac{P_i(1)\cdot p_{i_o}}{q_f \cdot l} \quad \text{(Eq. 13)} \qquad P_i' = \frac{P_i(X)}{P_i(1)} \quad \text{(Eq. 14)}$$

where q_f is the feed flow (mol/s), $P_i(1)$ is the permeability of the pure substance (mol s^{-1} m^{-1} Pa^{-1}) and $P_i(X)$ is the permeability of interest, in other words, the permeability of the permeating substance given a molar fraction (mol s^{-1} m^{-1} Pa^{-1}).

Combining the mass balances, the three dimensionless numbers and Eq. 2 (that corresponds to one of the equations of β_{ij}) the following ordinary differential equations (ODE) appear:

$$\text{ODE 1:} \quad \frac{dq\prime}{dX} = \frac{q'\left(X+\frac{1-X}{\beta_{ij}}\right)}{X(1-X)\left(1-\frac{1}{\beta_{ij}}\right)} \quad \text{(Eq. 15)}$$

$$\text{ODE 2:} \quad \frac{dS\prime}{dX} = \frac{-q\prime}{P_i' \cdot X\,(1-X)\left(1-\frac{1}{\beta_{ij}}\right)} \quad \text{(Eq. 16)}$$

This differential equation system will be solved using the Euler ODE resolution method. First, some initial and final boundary conditions must be defined: at the beginning, $X=X_f$, $S'=0$ and $q'=1$;

and at the end, X=X_r, $S' = S_T \frac{P_i(1) \cdot p_{i_o}}{q_f \cdot l}$ and q'=1-θ. S_T corresponds to the total permeating surface, which is 0.294 m^2, and $P_i(1)$ has already been calculated. Secondly, columns containing molar fractions from X_f to X_r (the smaller the increments, the more precise the results will be) and q' from $q' = q_f/q_f = 1$ to $q' = \frac{q_f}{q_f} = 1 - \theta$ are made. Additionally, a column with supposed β_{ij} and another with $\Delta q'/\Delta X$ values (obtained with Eq.15) are also made. Since the first q' value is known, the first $\Delta q'/\Delta X$ and then the second q' values can be calculated. Reiterating this process, all the columns are filled. The correct β_{ij} appear when the last q' is equal to its final boundary condition, so β_{ij} values should be modified until this happens. This last step can be done using the "solver" tool on the last q' value, defining the final boundary condition value as the objective. The final β_{ij} is the average of all the values. For the calculation of P_i' the process used is the same: Supposed values are assigned to P_i' and a column with $\Delta S'/\Delta X$ values (calculated with Eq.16) is made. Like q', the first S' value is known. Consequently, the first $\Delta S'/\Delta X$ and then the second S' values can be calculated. When the columns are filled by reiterating this process, a final S' is obtained. P_i' values must be modified until S' equals its final boundary condition. Once again, "solver" can be applied on the las S' value, defining as objective its final boundary condition. The final P_i' is the average of all the values.

Alternatively, both β_{ij} and P_i' columns can be replaced by a single value that will be used in every calculation of the two ODE, instead of depending on a different β_{ij} on every composition value. Either with constant or multiple β_{ij} and P_i', values obtained are almost the same, being the difference noticeable only from the fourth decimal. For example, β_{ij} and P_i' for the experiment X_m=0.90 48R1 are 1.2045766 and 0.90793 respectively for multiple values and 1.2045767 and 0.90794 respectively for a single value. As it can be appreciated, β_{ij} changes at the seventh decimal and P_i' at the fifth.

Finally, once β_{ij} and P_i' have been calculated, Eq. 14 must be applied on P_i' to obtain the permeability (P_i). The Pi(1) used must be the one that corresponds to that experiment's pump configuration.

4. RESULTS AND DISCUSSION

4.1. ACETONE-WATER MIXTURES

For the separation of acetone from aqueous mixtures through pervaporation, the influence of acetone feed molar fraction (X_f) and feed flow rate (q_f) has been studied. The parameters evaluated for these effects are the following: molar fraction in the permeate side (Y_p), product recovery fraction (θ), total feed percentage that has permeated, percentage of acetone that has permeated, separation factor (β_{ij}) and permeability (P_i).

Before proceeding with the discussion, some clarifications must be highlighted:

- In all the graphics the values plotted are the average of the three replicates in order to make data more significant from a statistical point of view.
- The graphics shown may be one representative example of the multiple configurations/conditions performed.
- All the experiments that present a Y_p greater than one (and consequently incoherent β_{ij} values), which is impossible, have already been discarded. No apparent reason can be deduced since this had happened at low and high q_f and X_f (these experiments are X_m= 0.75 48R2, X_m= 0.75 40R1, X_m= 0.05 20R2 and X_m= 0.01 48R2).
- Feed flow values may have an error of 1.52% due to the volume occupied by the silicone tube.
- As it can be seen comparing Table A4 and Table A8 most of the experiments' permeabilities are bigger than pure acetone permeabilities. This may look impossible since the membrane is hydrophobic, meaning that theoretically the maximum flux should be achieved with pure acetone, but all experiments have been done under the same procedure, so the reliability of the results, corresponding to at least triplicated experiments, is not questioned. Further work is recommended to comprehend this phenomenon from a physiochemical point of view.

- Parameter values at minimum concentrations may differ from the observed general trends due to the limitations that working with such small molar fractions represent.
- In β_{ij} graphics both experimental and calculated values are plotted. Experimental β_{ij} calculation has already been explained, and the calculated values are determined using Eq. 3 with Y_p and X_f values, showing what separation factors should be expected given these compositions.

4.1.1. Evaluation of the influence of X_f on relevant pervaporation parameters

a) Permeate molar fraction (Y_p)

As shown in Figure 14, Y_p increases, as it was expected, with feed concentration. The more the acetone that is fed, the more will permeate, translating in a raise in the permeate concentration. Additionally, it can be noticed that in the low X_f range the permeate concentration grows in a higher rate. Since the separation factor in all the experiments surpasses the unit, acetone will preferentially permeate, meaning that Y_p will always be higher than X_f. However, at a high feed concentration range values seem to remain constant given that such a high concentration gradient is not possible. This transition occurs approximately at X_f= 0.200 for the 48 and 40 rpm configurations, at 0.400 for the 30 rpm configuration and at high composition range for the 20 rpm configuration, remaining all constant at approximately Y_p= 0.85.

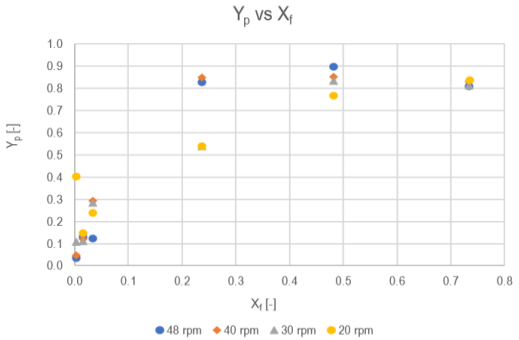

Figure 14. Permeate acetone molar fraction (Y_p) vs Feed acetone molar fraction (X_f)

b) Product recovery fraction (θ)

Product recovery fraction corresponds to the quotient of the permeate flow (q_p) by feed flow (q_f). A change in X_f significantly influences q_p. due to the higher amount of acetone available to permeate. In the other hand, q_f decreases with X_f (Figure A4) since the presence of more acetone translates to less total mols: for a same feeding volume, the higher the acetone concentration, the less total mass will be fed due to acetone's lower density and, moreover, total fed mols decrease with acetone mass because its molecular weight is bigger than water's. In conclusion, θ increases with feed concentration.

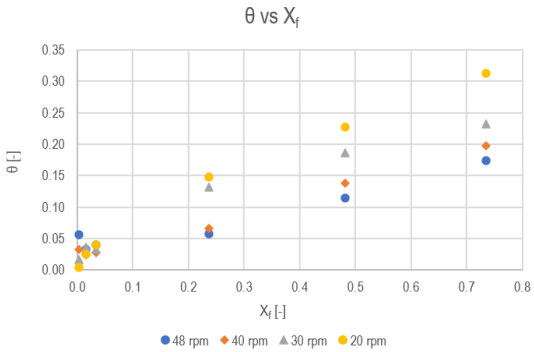

Figure 15. Product recovery fraction (θ) vs feed acetone molar fraction (X_f)

c) Total permeate percentage

This percentage refers to the total amount of feed that has permeated, including both water and acetone. As it can be observed in Figure 16, the total amount of permeate increases with increasing acetone concentration in the feed stream. The hydrophobic characteristics of the membrane allow acetone to permeate over water, so if acetone fraction in the feed increases the permeate flux will increase as well.

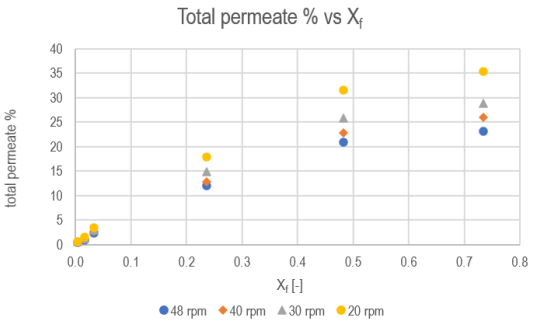

Figure 16. Total permeate percentage vs feed acetone molar fraction (X_f)

d) Permeated acetone percentage

Figure 17 show how the percentage of acetone permeated is almost constant for different feed concentrations. At the minimum X_f this percentage increases drastically in all four pump configurations, but an imprecision in sample taking is attributed since such small concentrations can easily vary with a minimum change. In conclusion, X_f barely affects the percentage of acetone that has permeated. There is more acetone present in the feed when X_f increases, but there is not any force that makes this percentage increase. However, an effect of feed flow can be perceived, but it will be discussed later.

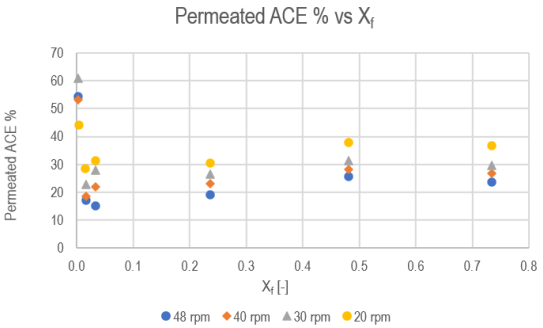

Figure 17. Permeated ACE percentage vs feed acetone molar fraction (X_f)

e) Separation factor (β_{ij})

In all four pump configurations is observable that separation factor decreases with feed concentration. This fall accentuates at low X_f, and almost remain constant when high X_f are approached. At low concentrations a big gradient between X_f and Y_p is still possible while at big concentrations it is not. β_{ij} corresponds to the concentration relationship between the feed and the permeate, so it will increase when a higher concentration gradient is achieved. As water fraction gets smaller, it is more difficult for the membrane to separate it, then becoming less selective. However, although β_{ij} decreases as well, at 48 rpm pump configuration it does not do it under the same fashion. X_m= 0.75 and 0.50 values should be lower so an imprecision in sample taking must have been done. It is remarkable that the experimental values of β_{ij} are very similar to the calculated ones, differing the most at low concentrations. The rest of representations are shown in Figures A5 to A7.

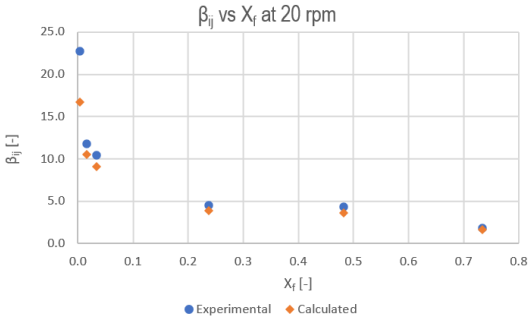

Figure 18. Separation factor (β_{ij}) vs feed acetone molar fraction (X_f) in the 20 rpm pump configuration

f) Permeability (P_i)

Permeability is a component flux normalized for membrane thickness and driving force, meaning that their effects are removed [10]. This is why the representations of P_i vs X_f are almost constant whereas the representations of J_i vs X_f show a positive-slope line (flux offer permeation rate information through the membrane but, unlike permeability, the effects of the driving force (pressure gradient) are not removed), as seen in Figure 20.

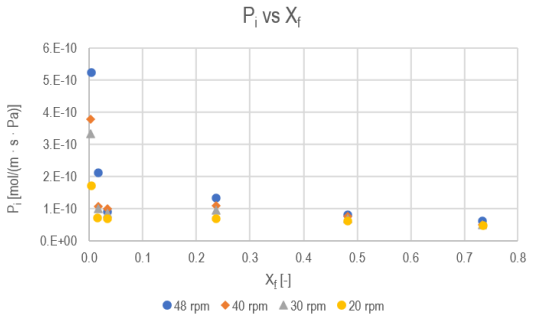

Figure 19. Permeability (P_i) vs feed acetone molar fraction (X_f)

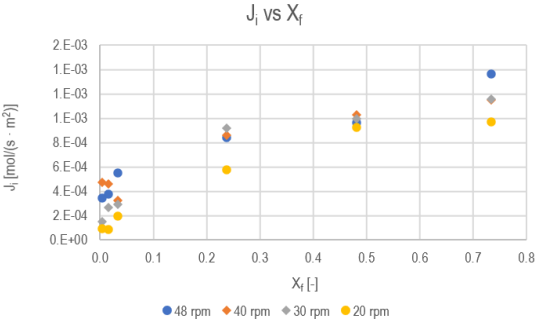

Figure 20. Total flux (J_i) vs feed acetone molar fraction (X_f)

4.1.2. Evaluation of the influence of q_f on relevant pervaporation parameters

a) Permeate molar fraction (Y_p)

Increasing the feed flow rate, and consequently the flux, leads to a higher penetration rate of the molecules in the membrane. Consequently, its hydrophobic properties increase as well, being more selective and therefore increasing Y_p with increasing feed flow rate. However, at low concentrations this trend is not observed to the limitations that working with such small molar fractions represent.

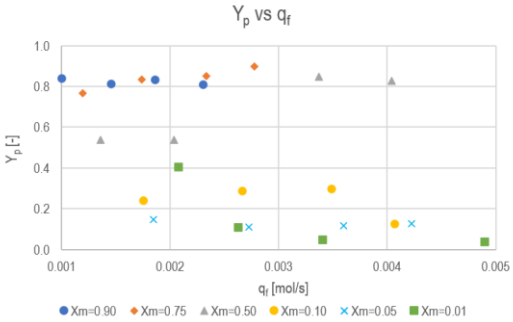

Figure 21. Permeate acetone molar fraction (Y_p) vs feed flow (q_f)

b) Product recovery fraction (θ)

Unlike with feed concentration, θ decreases with feed flow. In this case, q_p also increases since there are more acetone mol/s available to permeate, but it does not at the same rate. At a higher speed, it becomes more difficult for the acetone molecules to adsorb through the membrane. In other words, permeate flow does increase but its relationship with feed flow decreases. In the X_m= 0.01 experiments is just the opposite, but experimental imprecisions will be attributed since the other five compositions follow this fashion.

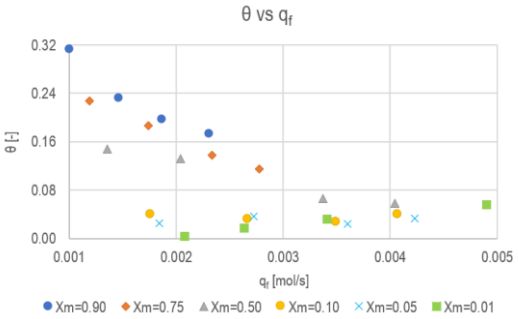

Figure 22. Product recovery fraction (θ) vs feed flow (q_f)

c) Total permeate percentage

Following product recovery fraction explanation, higher flow rates imply more difficulties for the molecules to adsorb on the membrane. Flow rate will increase, but not the total amount of permeate. That is why permeate percentage decreases with feed flow, as shown in Figure 23.

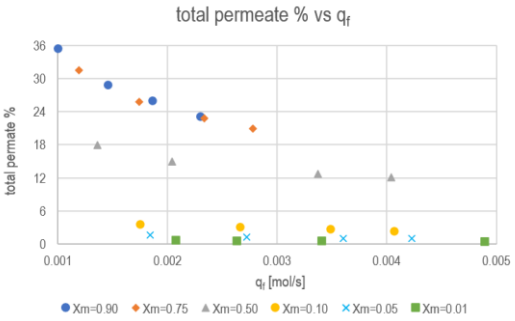

Figure 23. Permeate percentage vs feed flow (q_f)

d) Permeated acetone percentage

Unlike feed composition, feed flow does affect the percentage of acetone that has permeated. Its trend is to decrease with qf, such as θ and permeate percentage, being the reason that while acetone quantity in the feed is the same (concentration remains constant in these representations), its total permeated amount will decrease (although permeate flow increases) due the mentioned difficulties for the molecules to adsorb through the membrane.

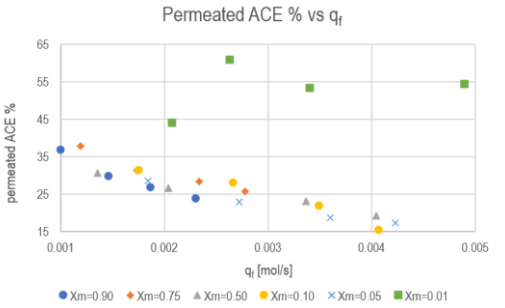

Figure 24. Permeated ACE percentage vs feed flow (q_f)

e) Separation factor (β_{ij})

Feed flow is supposed to enhance the separation factor, however, in the experiments assessed, this trend is only visible for feed molar fractions of 0.75, 0.50 and 0.05. For the other three compositions (X_m= 0.90, 0.10 and 0.01) there is not an extrapolatable trend, some values fall and some increase. With this being said, although further studies could be done on the effects of q_f in β_{ij} to be more certain, this increasing trend in the majority of X_f was already expected: if increasing feed flow poses difficulties for acetone to permeate, it does even more for water, which is not the preferential substance. This means that the selective properties of the membrane increase, hence β_{ij} does as well. The rest of representations are shown in Figures A8 to A12.

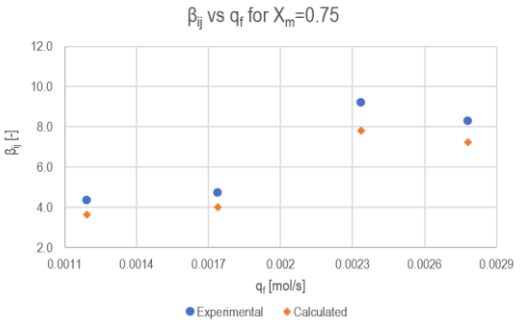

Figure 25. Separation factor (β_{ij}) vs feed flow (q_f) for X_m=0.75

f) Permeability (P_i)

Permeability, despite being a normalized parameter, does vary with feed flow. P_i depends on the permeate flux, membrane thickness and pressure gradient (driving force). Given a certain pressure gradient and being the membrane thickness constant, flux can indeed change P_i, so if a rise of qf, and consequently flux, is applied permeability will also increase, as shown in Figure 26.

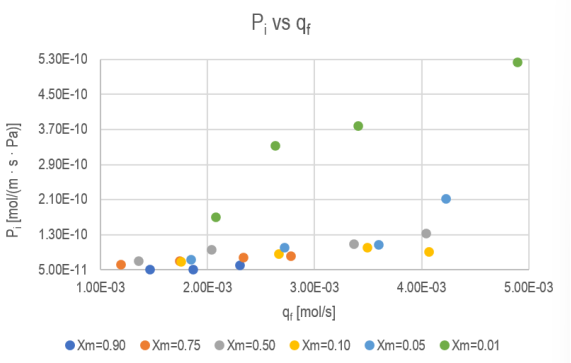

Figure 26. Permeability (P_i) vs feed flow (q_f)

4.1.3. General overview and optimum separation parameters

After assessing the effects of feed composition and feed flow rate on PV for the separation of acetone from aqueous mixtures in detail, the configurations of X_f and q_f to optimise the parameters assessed can be inferred:

- Permeate molar fraction (Y_p): although above a specific concentration it remains almost constant, increases with X_f and with q_f. Since at high feed flow rates the point above from Y_p remains constant is approximately at X_f= 0.200, optimal permeate molar fraction values are obtained at any X_f above this one and high q_f.
- Product recovery fraction (θ): increases with feed concentration but decreases with feed flow. This means optimal values are obtained at high at X_f and low q_f.
- Permeate percentage: like θ, optimal values are obtained at high at X_f and low q_f.
- Permeated acetone percentage: X_f does not influence it but it does decrease with q_f. Optimal values are obtained at any feed concentration and at low feed flows.
- Separation factor (β_{ij}): decreases with feed composition and increases with feed flow. Optimal values are obtained at low X_f and high q_f.
- Permeability (P_i): X_f does not have an influence but qf does. P_i increases with feed flow, meaning optimal values are obtained at any X_f and high q_f.

Although high X_f offer optimal values in five of the factors, P_i can obtain them as well at low concentrations. β_{ij} is the one that can only obtain them at low X_f, and since these two factors are the most important ones regarding PV efficiency, low X_f are the best in terms of pervaporation performance.

High qf values offer optimal values in three factors, being these ones Permeate molar fraction (Y_p), separation factor (β_{ij}) and permeability (P_i). Regarding their importance, high q_f are the best to achieve high PV efficiency.

4.2. PURE ORGANIC SOLVENTS

Permeabilities of some pure organic solvents have been studied as well at the higher pump configuration (48 rpm). These are methanol, ethanol, 1-butanol and methyl *tert*-butyl ether (MTBE). However, MTBE experiments could not be carried out due to experimental setup impediments. The silicone membrane absorbs the solvent in such a way that it almost doubles its thickness, becoming not suitable for the peristaltic pump used since the silicone tube breaks almost when the experiment has just started. However, methanol, ethanol and 1-butanol permeabilities have been successfully determined.

The three primary alcohols studied are less volatile than acetone (at the operating temperatures, their vapour pressures are approximately 16 kPa for methanol, 7 kPa for ethanol and 0,9 kPa for 1-butanol while acetone vapour pressure is approximately 30 kPa), meaning that in order to achieve a considerable pressure gradient vacuum pressure has to be even lower. The vacuum pressure provided by the vacuum pump used cannot be manipulated, having values that go from 9 kPa to 11 kPa. These are bigger than ethanol and 1-butanol vapour pressures, so their driving force gradient is negative and consequently so are their permeabilities. The only substance that should permeate since it has a positive pressure gradient is MeOH, as shown in Table A5.

Although EtOH and BuOH permeabilities seem to be negative, there still was permeate flux. Its explanation is the following: In a vacuum cell it is impossible to achieve absolute vacuum since

there always are small orifices through which air particles can flow. p_{il} (parameter involved in P_i calculation) is actually the partial pressure of the substance, not the total vacuum pressure indicated by the vacuum meter. As it is impossible to differentiate the permeated solvent's partial pressure and the one applied by this unwanted air particles, total vacuum pressure is used but in reality the pressure involved in P_i calculation is way lower, then achieving a positive pressure gradient that lets the solvent permeate. In order to show comparable data, permeabilities have been recalculated with an arbitrary, low enough partial pressure (100 Pa) so that the pressure gradients become positive for all the solvents used (Table A6).

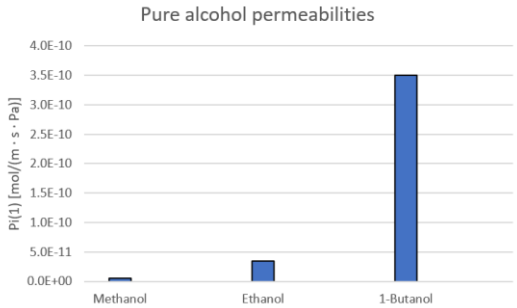

Figure 27. Permeabilities (P_i) of pure methanol, ethanol and 1-butanol with an arbitrary p_{il}

Flux seems to increase with bigger molecules, being the 1-butanol flux the biggest and methanol flux the smallest. In the other hand, pressure gradient decreases with molecule size due to smaller vapour pressures, but they are all in the same magnitude order while MeOH and BuOH fluxes have different ones. This leads to a higher permeability for 1-butanol upon ethanol and methanol, being all three Pi in different magnitude orders (P_i is 4.94E-12 mol/(m·s·Pa) for methanol, 3.50E-11 mol/(m·s·Pa) for and 3.50E-10 mol/(m·s·Pa) for 1-butanol). According to LaPack *et al.* [29], permselectivity for a substance in a silicone membrane is determined predominantly by the relative solubilities, increasing its permeability with solubility. The results obtained in this work are in good agreement with the values reported by LaPack *et al.* since MeOH, EtOH and BuOH solubilities (in mL/(cm^3 membrane·cmHg)) are 13, 28 and 29 respectively, proving that P_i does indeed increase with solubility.

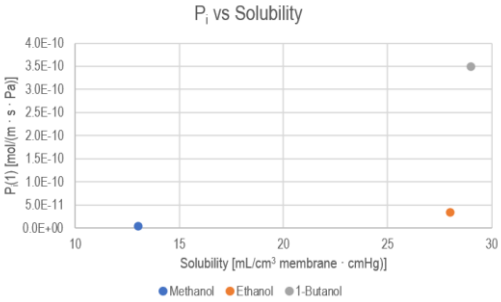

Figure 28. Alcohol permeabilities (P_i) calculated with an arbitrary p_{il} vs Solubility

Hildebrand solubility parameter can also be used for comparison, in this case being inversely proportional to P_i. The authors have observed that permeability of a solvent is higher when its Hildebrand solubility parameter is closer to the membrane's parameter (their solubility parameter relation is 1). Silicone has a solubility parameter (in $(J/cm^3)^{1/2}$) of 19.2 and methanol, ethanol and 1-butanol have a solubility parameter of 29.7, 26.0 and 23.0, respectively. The alcohol that has the closest solubility parameter to the silicone's parameter is 1-butanol, meaning that it should have the highest P_i, as proven experimentally. In the other hand, methanol has the lowest P_i since it has the furthest solubility parameter from the silicone parameter.

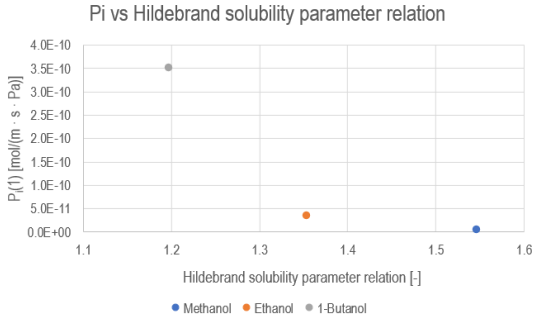

Figure 29. Alcohol permeabilities (P_i) calculated with an arbitrary p_{il} vs Hildebrand solubility parameters relative to the silicone solubility parameter

A further comparison including acetone can also be made by relating P_i with the Hansen solubility parameter (HSP)(physicochemical parameters used to estimate the type of interactive

forces responsible for compatibility between materials [30]), which takes into account the Hildebrand solubility parameter, being as well inversely proportional to P_i. HSP for MeOH, EtOH and BuOH are 49.7, 44.0 and 36.7 respectively. Acetone has an HSP of 32.9, meaning that it should have a higher P_i than 1-butanol. However, experimental data show that BuOH permeability is considerably higher, opposing the expected trend. With this in mind, studies with larger amount of replicates are recommended to be done.

These correlations with solubility parameters indicate that permeability does not only depend on feed flow or feed composition, but also on the chemical nature of the solvents used.

4.3. ABE FERMENTATION PROCESS BLEND

Finally, pervaporation performance for the separation of a representative composition of the ABE fermentation process (30% ACE, 60% BuOH and 10% EtOH, in w/w) was studied. In this case, results are given in GC Area % since a composition calibration of a ternary mixture is complicated to do. However, this parameter still allows to evaluate PV performance in a qualitative way comparing the initial GC area percentage values and the retained portion ones.

Both 1-butanol and ethanol percentages are higher in the retained portion, increasing its percentage 21.8% for BuOH and 7.1% for EtOH. In the other hand, acetone GC area % is smaller in the retained portion, reducing the percentage a 42.8%. Water percentage seem to decrease as well, probably because their molecules are dragged through the membrane by the permeated acetone since water should not permeate. Even though its variation is negligible.

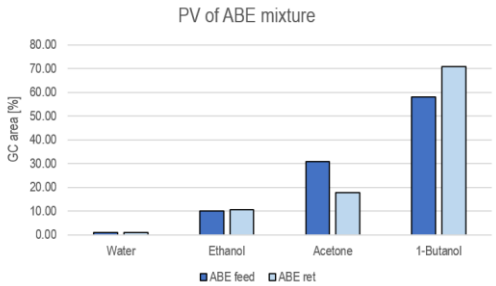

Figure 30. GC area % of an ABE mixture and its retained portion

That EtOH and BuOH percentages in the retained portion increases while acetone's decreases means that acetone's Y_p is bigger than its feed fraction, and therefore is preferentially permeating through the membrane. Ethanol and 1-butanol might permeate as well, but not at the same rate as acetone does (GC area % would be the same in the retained portion if this happened). With this information it can be concluded that acetone permeates selectively through a SC membrane in presence of ethanol and 1-butanol, meaning that PV is a valid process for the separation of acetone from an ABE fermentation process blend.

5. CONCLUSIONS

It can be concluded that all the objectives have been targeted successfully:

- Several modifications of the experimental set up have been undertaken in order to maximize the amount the amount of permeate that can be collected from the setup as condensed phase. Cooling has been found to be the main restriction within the explored conditions and hence the setup enable the partial condensation of the permeate given the limitations of cooling devices available in the lab. This would not be a problem from an industrial standpoint where temperatures as low as -96 ^{o}C are easily attainable.
- Pervaporation performance of a silicone composite (SC) membrane-type for separating acetone-water mixtures has been studied by comparing permeabilities and separation factors under different feed compositions and feed flow rates. Optimum pervaporation parameter values have been obtained at low X_f and high q_f, being these the optimal operating conditions.
- Different techniques for composition determination have been assessed. These include refractometry, UV-vis absorption and gas chromatography, concluding that gas chromatography is the best technique given its operating simplicity, reproducibility and reliability.
- Although MTBE experiments could not be performed due to experimental complications, permeabilities of methanol, ethanol and 1-butanol have been determined. Among them, BuOH showed the highest P_i and MeOH the lowest due to increasing solubility or decreasing Hildebrand solubility parameter or HSP. Acetone, however, did not follow this trend. Such correlation with the solubility parameters indicates that the same interactions at play in the dissolution process between acetone and the studied solvents also play a determinant role in the pervaporation process. This finding constitutes a starting point for further studying the permeability of the silicone membrane in further solvent, with the consequent prospective of tailoring a membrane for the separation of specific mixtures.

- Pervaporation through a silicone membrane results successful for the separation of acetone from streams with a representative composition of the ABE fermentation process.
- A reproducible experimental procedure using an improved set up has been established in order to develop a possible Chemical Engineering degree lab practice.

REFERENCES AND NOTES

[1] *GREEN AND SUSTAINABLE CHEMISTRY: FRAMEWORK MANUAL*. [Online]. Available: https://www.unenvironment.org/explore-topics/chemicals-waste

[2] L. Kahklekberg, "General and Physical Chemistry," *Journal of Physical Chemistry*, vol. 10, pp. 141–209, 1906.

[3] P. A. Kober, "Pervaporation, perstillation and percrystallization," *J Am Chem Soc*, vol. 39, no. 5, pp. 944–948, May 1917, doi: 10.1021/JA02250A011/ASSET/JA02250A011.FP.PNG_V03.

[4] P. Aptel, N. Challard, J. Cuny, and J. Neel, "Application of the pervaporation process to separate azeotropic mixtures," *J Memb Sci*, vol. 1, no. C, pp. 271–287, Jan. 1976, doi: 10.1016/S0376-7388(00)82272-3.

[5] R. C. Binning, R. J. Lee, J. F. Jennings, and E. C. Martin, "Separation of liquid mixtures by permeation," *Preprints (Basel)*, vol. 3, no. 1, pp. 131–141, 1958, doi: 10.1021/IE50613A030/ASSET/IE50613A030.FP.PNG_V03.

[6] S. Sridhar, S. Moulik, "Membrane Processes: Pervaporation, vapor permeation and membrane distillation for industrial scale separations", 2019. [Online]

[7] A. Basile, A. Figoli, and M. Khayet, "Woodhead Publishing Series in Energy: Number 77 Pervaporation, Vapour Permeation and Membrane Distillation Principles and Applications," 2015. [Online]. Available: http://store.elsevier.com/

[8] M. H. V. Mulder and C. A. Smolders, "On the mechanism of separation of ethanol/water mixtures by pervaporation I. Calculations of concentration profiles," *J Memb Sci*, vol. 17, no. 3, pp. 289–307, Feb. 1984, doi: 10.1016/S0376-7388(00)83220-2.

[9] T. Okada and T. Matsuura, "A new transport model for pervaporation," *J Memb Sci*, vol. 59, no. 2, pp. 133–149, Jun. 1991, doi: 10.1016/S0376-7388(00)81179-5.

[10] R. W. Baker, J. G. Wijmans, and Y. Huang, "Permeability, permeance and selectivity: A preferred way of reporting pervaporation performance data," *J Memb Sci*, vol. 348, no. 1–2, pp. 346–352, Feb. 2010, doi: 10.1016/j.memsci.2009.11.022.

[11] P. L. C. M. B. F. O. S. N. S. S. H. W. M. and C. M. R. H. Bello, "Pervaporation of ethanol produced from banana waste," *Waste Management*, vol. 34, pp. 1501–1509, 2014.

[12] A. K. D. and S. P. C. A. Jain, *International Journal of Research and Scientific Innovation*, vol. 4. 2017.

[13] S. Moulik, K. P. Kumar, S. Bohra, and S. Sridhar, "Pervaporation performance of PPO membranes in dehydration of highly hazardous mmh and udmh liquid propellants," *J Hazard Mater*, vol. 288, pp. 69–79, May 2015, doi: 10.1016/J.JHAZMAT.2015.02.020.

[14] R. Wilson *et al.*, "Influence of Clay Content and Amount of Organic Modifiers on Morphology and Pervaporation Performance of EVA/Clay Nanocomposites," *Ind Eng Chem Res*, vol. 50, no. 7, pp. 3986–3993, Apr. 2011, doi: 10.1021/IE102259S.

[15] "(Micro and Nano Technologies) Sabu Thomas (editor), Soney C. George (editor), Thomasukutty Jose (editor) - Polymer Nanocomposite Membr".

[16] M. N. Hyder, R. Y. M. Huang, and P. Chen, "Effect of selective layer thickness on pervaporation of composite poly(vinyl alcohol)–poly(sulfone) membranes," *J Memb Sci*, vol. 318, no. 1–2, pp. 387–396, Jun. 2008, doi: 10.1016/J.MEMSCI.2008.03.002.

[17] S. Biduru, S. Sridhar, G. S. Murthy, and S. Mayor, "Pervaporation of tertiary butanol/water mixtures through chitosan membranes cross-linked with toluylene diisocyanate," *Journal of Chemical Technology & Biotechnology*, vol. 80, no. 12, pp. 1416–1424, Dec. 2005, doi: 10.1002/JCTB.1347.

[18] S. G. Adoor, B. Prathab, L. S. Manjeshwar, and T. M. Aminabhavi, "Mixed matrix membranes of sodium alginate and poly(vinyl alcohol) for pervaporation dehydration of isopropanol at different temperatures," *Polymer (Guildf)*, vol. 48, no. 18, pp. 5417–5430, Aug. 2007, doi: 10.1016/J.POLYMER.2007.06.064.

[19] L. Y. Jiang, T. S. Chung, and R. Rajagopalan, "Matrimid®/MgO mixed matrix membranes for pervaporation," *AIChE Journal*, vol. 53, no. 7, pp. 1745–1757, Jul. 2007, doi: 10.1002/AIC.11198.

[20] X. Liu *et al.*, "Metal–organic framework ZIF-8 nanocomposite membrane for efficient recovery of furfural via pervaporation and vapor permeation," *J Memb Sci*, vol. 428, pp. 498–506, Feb. 2013, doi: 10.1016/J.MEMSCI.2012.10.028.

[21] V. Muthukumaraswamy Rangaraj *et al.*, "Metal Organic Framework — Based Mixed Matrix Membranes for Carbon Dioxide Separation: Recent Advances and Future Directions," *Front Chem*, vol. 8, p. 534, Jul. 2020, doi: 10.3389/FCHEM.2020.00534/BIBTEX.

[22] H.L. Fleming and C.S. Slater, "Pervaporation," *Membrane Handbook*, p. 105, 1992.

[23] S. Sridhar, S. Moulik, "Membrane Processes: Pervaporation, vapor permeation and membrane distillation for industrial scale separations", 2019. [Online]

[24] and S. D. D. N.G. Kanse, “International Journal of Engineering Sciences & Research Technology,” vol. 4(12). pp. 472–479, 2015.

[25] C. T. T. and S. B. S.L.Wee, “Separation and Purification Technology,” vol. 63. pp. 500–516, 2008.

[26] E. A. Buehler and A. Mesbah, “Kinetic Study of Acetone-Butanol-Ethanol Fermentation in Continuous Culture,” *PLoS One*, vol. 11, no. 8, Aug. 2016, doi: 10.1371/JOURNAL.PONE.0158243.

[27] C.-A. L. J. G. M. L. E. T. D. and A. P. H. Victoria Outram, “Applied in situ prodcut recovery in ABE fermentation,” *Biotechnol Prog*, vol. 33(3), pp. 563–579, Mar. 2017.

[28] S. Belletante, L. Montastruc, S. Negny, and S. Domenech, “Optimal design of an efficient, profitable and sustainable biorefinery producing acetone, butanol and ethanol: Influence of the in-situ separation on the purification structure,” *Biochem Eng J*, vol. 116, pp. 195–209, Dec. 2016, doi: 10.1016/J.BEJ.2016.05.004.

[29] M. A. LaPack, J. C. Tou, V. L. McGuffin, and C. G. Enke, “The correlation of membrane permselectivity with Hildebrand solubility parameters,” *J Memb Sci*, vol. 86, no. 3, pp. 263–280, Feb. 1994, doi: 10.1016/0376-7388(93)E0155-D.

[30] C. M. Hansen, “8 The Future,” 2007.

ACRONYMS

ACE	Acetone
E_a	Activation energy
BuOH	Butanol
P	Density
D_i	Diffusion coefficient
EtOH	Ethanol
D_2	External tube diameter
v	Fluid velocity
J_i	Flux
GC	Gas chromatography
R_g	Gas constant
HSP	Hansen solubility Parameter
D_1	Internal tube diameter
D_{ml}	Logarithmic mean diameter
X_m	Mass fraction
S	Membrane surface
l	Membrane width
MOFs	Metal organic frameworks
MeOH	Methanol
MTBE	Methyl tert-butyl ether
MMMs	Mixed matrix membranes

q_f	Molar feed flow
q	Molar flow
X	Molar fraction in liquid phase
X_f	Molar fraction in the feed portion
Y_p	Molar fraction in the permeate portion
X_r	Molar fraction in the retained portion
Y	Molar fraction in the vapour phase
P_{il}	Partial pressure/vacuum pressure
P_i	Permeability
P/l	Permeance
q_p	Permeate flow
PV	Pervaporation
PDMS	Polydimethylsiloxane
θ	Product recovery fraction
q_r	Retentate flow
α_{ij}	Selectivity
β_{ij}	Separation factor
SC	Silicone composite
S_i	Sorption coefficient
T	Temperature
P_{io}	Vapour pressure
μ	Viscosity
VOCs	Volatile organic compounds

Appendices

APPENDIX 1: ANALYSIS EQUIPMENT CALIBRATION

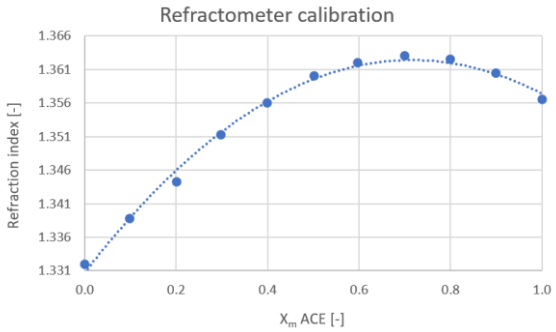

Figure A1. Refractometer calibration – Refraction index vs feed acetone mass fraction (X_m)

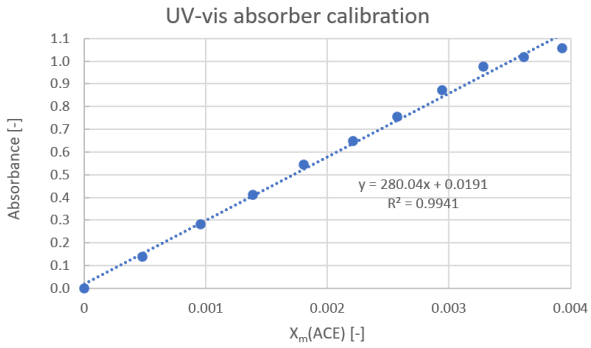

Figure A2. UV-vis absorber calibration – Absorbance vs feed acetone mass fraction (X_m)

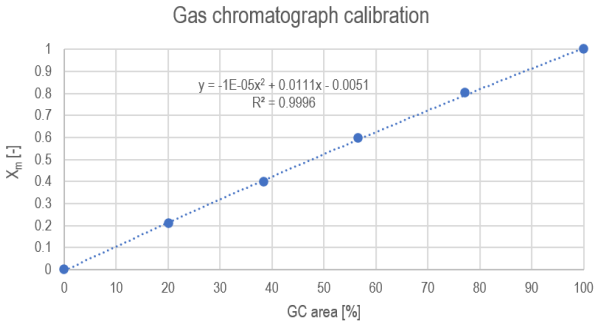

Figure A3. Gas chromatograph calibration - Feed acetone mass fraction (X_m) vs GC area percentage

APPENDIX 2: ACETONE-WATER MIXTURES EXPERIMENTAL DATA

Table A1. Example of experimental data obtained in one experiment (X_m=0.90 and 48 rpm)

R1					
Vacuum pressure [mbar]			125		
Temperature [ºC]			20		
Feed (approx. 100 mL) [g]		81.22	ACE in jar with water [g]		8.30
ACE fed [g]		73.03	Condensed [g]		6.78
Water fed [g]		8.19	% Recovered permeate		18.57
Retentate [g]		62.80			
Retentate [%]		77.32			
Leaked mass [g]			3.34		
Leaked mass [%]			4.11		
Feed			Retentate		
Time when it finishes [min]		17.47	Time when it starts [min]		9.42
Volumen fed [mL]	time [min]	q [mL/min]	Volume retained [mL]	time [min]	q [mL/min]
10	1.78	5.61	10	2.17	4.62
20	3.58	5.58	20	4.33	4.62
30	5.37	5.59	30	6.53	4.59
40	7.07	5.66	40	8.67	4.62
50	8.77	5.70	50	13.33	3.75
60	10.50	5.71	60	17.50	3.43
70	12.27	5.71	70	22.40	3.13
80	14.00	5.71	80	-	-
90	15.80	5.70	90	-	-
100	17.47	5.73	100	-	-
q average [mL/s]		9.45E-02	q average [mL/s]		7.68E-02

Table A2. Experimental data summary

			p_{il} [Pa]	Permeate [%]	ACE permeated [%]	X_f [-]	X_r [-]	Y_p [-]
X_m = 0,90	48 rpm	R1	12500	22.68	22.95	0.735	0.728	0.766
		R2	12400	23.39	24.05	0.735	0.718	0.812
		R3	14700	23.19	24.13	0.734	0.711	0.847
	40 rpm	R1	12900	24.08	24.42	0.735	0.726	0.769
		R2	14800	26.61	27.52	0.734	0.711	0.870
		R3	15100	26.98	28.06	0.734	0.706	0.848
	30 rpm	R1	12800	28.26	29.07	0.735	0.713	0.804
		R2	13000	29.60	30.22	0.734	0.717	0.791
		R3	14500	28.61	29.80	0.734	0.703	0.838
	20 rpm	R1	13000	37.30	38.67	0.735	0.694	0.821
		R2	12800	34.47	35.90	0.735	0.694	0.875
		R3	12600	34.30	35.52	0.735	0.7	0.813
X_m = 0,75	48 rpm	R1	13900	20.21	24.50	0.482	0.431	0.924
		R2	13700	20.96	26.23	0.482	0.42	1.229
		R3	14500	21.67	26.34	0.482	0.426	0.870
	40 rpm	R1	13800	22.05	29.04	0.482	0.4	1.123
		R2	13900	22.26	27.77	0.482	0.416	0.916
		R3	12500	23.93	28.07	0.482	0.431	0.787
	30 rpm	R1	13900	24.74	29.88	0.482	0.418	0.786
		R2	13900	25.26	30.58	0.482	0.416	0.922
		R3	14300	27.27	33.44	0.482	0.404	0.792
	20 rpm	R1	13800	31.12	37.31	0.482	0.4	0.759
		R2	13500	30.99	37.24	0.482	0.4	0.807
		R3	14000	32.43	38.81	0.482	0.396	0.735

Table A2. Experimental data summary (continued)

			p_{II} [Pa]	Permeate [%]	ACE permeated [%]	X_f [-]	X_r [-]	Y_p [-]
X_m = 0,50	48 rpm	R1	17000	12.08	28.48	0.237	0.175	0.926
		R2	17300	12.95	26.04	0.237	0.186	0.816
		R3	14000	11.15	19.12	0.237	0.206	0.743
	40 rpm	R1	16000	13.35	23.46	0.237	0.197	0.825
		R2	14000	12.39	20.65	0.237	0.204	0.514
		R3	13500	12.53	24.79	0.237	0.19	0.873
	30 rpm	R1	16000	14.90	26.87	0.237	0.189	0.543
		R2	17100	15.39	26.36	0.237	0.193	0.520
		R3	16500	14.43	26.33	0.237	0.19	0.553
	20 rpm	R1	15800	18.17	30.98	0.237	0.185	0.594
		R2	16700	17.28	30.15	0.237	0.185	0.847
		R3	16800	18.31	30.46	0.237	0.187	0.483
X_m = 0,10	48 rpm	R1	10400	2.34	6.46	0.034	0.032	0.069
		R2	10600	2.33	13.17	0.034	0.03	0.128
		R3	9700	2.17	17.30	0.033	0.028	0.173
	40 rpm	R1	10200	2.61	22.47	0.034	0.026	0.366
		R2	9300	2.59	22.55	0.033	0.026	0.233
		R3	9200	2.75	20.53	0.033	0.027	0.283
	30 rpm	R1	12000	2.96	26.82	0.034	0.025	0.334
		R2	9300	2.99	21.54	0.033	0.027	0.247
		R3	9400	2.97	28.88	0.033	0.024	0.275
	20 rpm	R1	11000	3.50	24.80	0.034	0.026	0.239
		R2	10700	3.35	33.39	0.034	0.023	0.675
		R3	10200	3.54	29.17	0.034	0.024	0.240
X_m = 0,05	48 rpm	R1	12900	0.88	29.98	0.016	0.011	0.160
		R2	12700	1.05	31.16	0.016	0.011	0.405
		R3	12800	1.02	17.22	0.016	0.014	0.098
	40 rpm	R1	14000	1.14	37.87	0.016	0.01	0.104
		R2	12800	0.97	36.58	0.016	0.01	0.270
		R3	13000	1.00	18.65	0.016	0.013	0.134
	30 rpm	R1	13500	1.27	25.54	0.016	0.012	0.289
		R2	13100	1.24	20.19	0.016	0.013	0.113
		R3	12800	1.30	22.87	0.016	0.013	0.105
	20 rpm	R1	13700	1.47	21.76	0.016	0.013	0.146
		R2	13100	1.42	28.79	0.016	0.011	1.076
		R3	13000	1.86	34.72	0.016	0.011	0.473
X_m = 0,01	48 rpm	R1	13500	0.15	12.25	0.004	0.003	0.077
		R2	14100	0.43	48.66	0.004	0.002	1.692
		R3	12700	0.39	60.05	0.003	0.001	0.035
	40 rpm	R1	14000	0.52	50.63	0.003	0.002	0.049
		R2	14200	0.51	60.85	0.003	0.001	0.037
		R3	12600	0.51	48.46	0.003	0.002	0.054
	30 rpm	R1	13400	0.55	55.43	0.004	0.002	0.080
		R2	13700	0.51	66.24	0.003	0.001	0.137
		R3	13200	0.56	79.39	0.003	0.001	0.259
	20 rpm	R1	13900	0.61	41.54	0.004	0.002	0.414
		R2	13500	0.62	39.31	0.004	0.002	0.390
		R3	13600	0.60	51.08	0.004	0.002	0.056

Table A3. Experimental data summary 2

			q_f [mol/s]	q_r [mol/s]	q_p [mol/s]	J_i [mol/(s · m^2)]	θ [-]
X_m = 0,90	48 rpm	R1	2.33E-03	1.91E-03	4.14E-04	1.41E-03	0.178
		R2	2.36E-03	1.95E-03	4.08E-04	1.39E-03	0.173
		R3	2.23E-03	1.85E-03	3.81E-04	1.30E-03	0.171
	40 rpm	R1	1.98E-03	1.59E-03	3.93E-04	1.34E-03	0.198
		R2	1.83E-03	1.56E-03	2.69E-04	9.16E-04	0.147
		R3	1.78E-03	1.43E-03	3.50E-04	1.19E-03	0.196
	30 rpm	R1	1.48E-03	1.13E-03	3.54E-04	1.21E-03	0.239
		R2	1.47E-03	1.14E-03	3.34E-04	1.14E-03	0.227
		R3	1.43E-03	1.10E-03	3.32E-04	1.13E-03	0.232
	20 rpm	R1	9.86E-04	6.71E-04	3.15E-04	1.07E-03	0.319
		R2	1.01E-03	7.82E-04	2.27E-04	7.71E-04	0.225
		R3	1.01E-03	7.02E-04	3.12E-04	1.06E-03	0.307
X_m = 0,75	48 rpm	R1	2.82E-03	2.53E-03	2.90E-04	9.87E-04	0.103
		R2	2.76E-03	2.55E-03	2.12E-04	7.22E-04	0.077
		R3	2.76E-03	2.41E-03	3.47E-04	1.18E-03	0.126
	40 rpm	R1	2.38E-03	2.11E-03	2.69E-04	9.17E-04	0.113
		R2	2.31E-03	2.00E-03	3.04E-04	1.04E-03	0.132
		R3	2.32E-03	1.98E-03	3.34E-04	1.14E-03	0.144
	30 rpm	R1	1.74E-03	1.44E-03	3.02E-04	1.03E-03	0.173
		R2	1.74E-03	1.52E-03	2.27E-04	7.74E-04	0.130
		R3	1.73E-03	1.38E-03	3.46E-04	1.18E-03	0.200
	20 rpm	R1	1.25E-03	9.66E-04	2.85E-04	9.72E-04	0.228
		R2	1.17E-03	9.34E-04	2.37E-04	8.07E-04	0.202
		R3	1.15E-03	8.62E-04	2.91E-04	9.92E-04	0.253
X_m = 0,50	48 rpm	R1	3.12E-03	2.86E-03	2.55E-04	8.69E-04	0.082
		R2	3.17E-03	2.91E-03	2.53E-04	8.62E-04	0.080
		R3	4.04E-03	3.81E-03	2.33E-04	7.93E-04	0.058
	40 rpm	R1	2.69E-03	2.52E-03	1.70E-04	5.80E-04	0.063
		R2	3.39E-03	3.04E-03	3.56E-04	1.21E-03	0.105
		R3	3.35E-03	3.12E-03	2.31E-04	7.87E-04	0.069
	30 rpm	R1	2.01E-03	1.74E-03	2.68E-04	9.14E-04	0.134
		R2	2.06E-03	1.79E-03	2.76E-04	9.39E-04	0.134
		R3	2.05E-03	1.78E-03	2.64E-04	9.00E-04	0.129
	20 rpm	R1	1.37E-03	1.19E-03	1.75E-04	5.94E-04	0.128
		R2	1.37E-03	1.26E-03	1.08E-04	3.66E-04	0.078
		R3	1.33E-03	1.11E-03	2.24E-04	7.64E-04	0.168
X_m = 0,10	48 rpm	R1	4.06E-03	3.89E-03	1.68E-04	5.72E-04	0.041
		R2	4.07E-03	3.91E-03	1.64E-04	5.59E-04	0.040
		R3	4.08E-03	3.93E-03	1.55E-04	5.26E-04	0.038
	40 rpm	R1	3.47E-03	3.39E-03	7.38E-05	2.51E-04	0.021
		R2	3.51E-03	3.38E-03	1.23E-04	4.20E-04	0.035
		R3	3.51E-03	3.42E-03	8.90E-05	3.03E-04	0.025
	30 rpm	R1	2.63E-03	2.55E-03	7.40E-05	2.52E-04	0.028
		R2	2.68E-03	2.60E-03	8.26E-05	2.81E-04	0.031
		R3	2.69E-03	2.59E-03	1.01E-04	3.44E-04	0.038
	20 rpm	R1	1.73E-03	1.66E-03	6.33E-05	2.16E-04	0.037
		R2	1.76E-03	1.73E-03	2.96E-05	1.01E-04	0.017
		R3	1.78E-03	1.70E-03	7.75E-05	2.64E-04	0.044

Table A3. Experimental data summary 2 (continued)

			q_f [mol/s]	q_r [mol/s]	q_p [mol/s]	J_i [mol/(s · m^2)]	θ [-]
X_m = 0,05	48 rpm	R1	4.23E-03	4.09E-03	1.37E-04	4.66E-04	0.032
		R2	4.22E-03	4.17E-03	5.46E-05	1.86E-04	0.013
		R3	4.23E-03	4.09E-03	1.39E-04	4.72E-04	0.033
	40 rpm	R1	3.60E-03	3.37E-03	2.33E-04	7.93E-04	0.065
		R2	3.60E-03	3.51E-03	8.32E-05	2.83E-04	0.023
		R3	3.60E-03	3.51E-03	8.97E-05	3.05E-04	0.025
	30 rpm	R1	2.73E-03	2.69E-03	3.98E-05	1.35E-04	0.015
		R2	2.72E-03	2.63E-03	8.74E-05	2.98E-04	0.032
		R3	2.72E-03	2.61E-03	1.08E-04	3.67E-04	0.040
	20 rpm	R1	1.84E-03	1.79E-03	4.64E-05	1.58E-04	0.025
		R2	1.85E-03	1.84E-03	7.90E-06	2.69E-05	0.004
		R3	1.84E-03	1.82E-03	2.23E-05	7.61E-05	0.012
X_m = 0,01	48 rpm	R1	4.98E-03	4.95E-03	2.91E-05	9.91E-05	0.006
		R2	4.93E-03	4.93E-03	5.02E-06	1.71E-05	0.001
		R3	4.79E-03	4.52E-03	2.69E-04	9.17E-04	0.056
	40 rpm	R1	3.43E-03	3.31E-03	1.18E-04	4.01E-04	0.034
		R2	3.39E-03	3.20E-03	1.85E-04	6.30E-04	0.055
		R3	3.98E-03	3.87E-03	1.17E-04	3.98E-04	0.029
	30 rpm	R1	2.57E-03	2.50E-03	6.39E-05	2.18E-04	0.025
		R2	2.57E-03	2.53E-03	4.00E-05	1.36E-04	0.016
		R3	2.76E-03	2.74E-03	2.72E-05	9.26E-05	0.010
	20 rpm	R1	2.08E-03	2.07E-03	7.39E-06	2.52E-05	0.004
		R2	2.10E-03	2.09E-03	7.48E-06	2.55E-05	0.004
		R3	2.06E-03	1.99E-03	6.84E-05	2.33E-04	0.033

APPENDIX 3: PURE SOLVENT PERMEABILITIES

Table A4. Pure acetone permeabilities

		q_f [mol/s]	q_r [mol/s]	J_i [mol/(m^2 · s)]	p_{il} [Pa]	T [ºC]	p_{io} [Pa]	$P_i(1)$ [mol/(m · s · Pa)]	average $P_i(1)$ [mol/(m · s · Pa)]
48 rpm	R1	9.60E-04	5.62E-04	1.35E-03	10500	25	30806	6.66E-11	6.58E-11
	R3	8.50E-04	4.33E-04	1.42E-03	9200	25	30806	6.57E-11	
	R4	8.39E-04	4.43E-04	1.35E-03	8700	24	29504	6.49E-11	
40 rpm	R3	7.27E-04	3.45E-04	1.30E-03	9200	25	30806	6.03E-11	6.01E-11
	R4	7.65E-04	3.80E-04	1.31E-03	8900	25	30806	5.98E-11	
30 rpm	R1	5.18E-04	1.55E-04	1.24E-03	11000	26	32154	5.85E-11	5.96E-11
	R2	5.31E-04	1.65E-04	1.25E-03	9000	24	29504	6.08E-11	
20 rpm	R1	3.31E-04	0.00E+00	1.13E-03	11000	25	30806	5.69E-11	5.72E-11
	R2	3.32E-04	0.00E+00	1.13E-03	9800	24	29504	5.74E-11	

Table A5. Parameters for the calculation of P_i of pure methanol, ethanol and 1-butanol

		q_f [mol/s]	q_r [mol/s]	J_i [mol/(m^2 · s)]	p_{il} [Pa]	T [ºC]	p_{io} [Pa]	$P_i(1)$ [mol/(m · s · Pa)]	average $P_i(1)$ [mol/(m · s · Pa)]
Methanol	R1	1.48E-03	1.45E-03	7.70E-05	8400	24	16055	1.01E-11	9.69E-12
	R2	1.53E-03	1.51E-03	8.07E-05	7400	24	16055	9.32E-12	
Ethanol	R1	1.13E-03	1.06E-03	2.36E-04	7600	23	6968	-3.74E-10	-4.54E-10
	R2	9.51E-04	8.84E-04	2.31E-04	7000	22	6568	-5.34E-10	
1-Butanol	R1	6.12E-04	5.37E-04	2.55E-04	6800	24	858	-4.30E-11	-4.46E-11
	R2	6.84E-04	6.03E-04	2.75E-04	6800	24	858	-4.62E-11	

Table A6. Parameters for the calculation of P_i of pure methanol, ethanol and 1-butanol with an arbitrary p_{il}

		q_f [mol/s]	q_r [mol/s]	J_i [mol/(m^2 · s)]	p_{il} [Pa]	T [ºC]	p_{io} [Pa]	$P_i(1)$ [mol/(m · s · Pa)]	average $P_i(1)$ [mol/(m · s · Pa)]
Methanol	R1	1.48E-03	1.45E-03	7.70E-05	100	24	16055	4.83E-12	4.94E-12
	R2	1.53E-03	1.51E-03	8.07E-05	100	24	16055	5.06E-12	
Ethanol	R1	1.13E-03	1.06E-03	2.36E-04	100	23	6968	3.44E-11	3.50E-11
	R2	9.51E-04	8.84E-04	2.31E-04	100	22	6568	3.57E-11	
1-Butanol	R1	6.12E-04	5.37E-04	2.55E-04	100	24	858	3.37E-10	3.50E-10
	R2	6.84E-04	6.03E-04	2.75E-04	100	24	858	3.63E-10	

APPENDIX 4: SEPARATION FACTORS AND PERMEABILITIES OF ACETONE-WATER MIXTURES

Table A7. Example of β_{ij} and P_i calculation for one experiment (X_m=0.90 and 48 rpm)

R1								
X [-]	q' [-]	θ [-]	β_{ij} [-]	Δq'/ΔX [-]	S' [-]	P_i' [-]	ΔS'/ΔX [-]	P_i [mol/(m · s · Pa)]
0.735	1.000	0.000		28.836	0.000		-33.259	
0.734	0.986	0.014		28.396	0.016		-32.755	
0.734	0.972	0.028		27.964	0.032		-32.259	
0.733	0.959	0.041		27.539	0.048		-31.771	
0.733	0.945	0.055		27.121	0.063		-31.291	
0.732	0.932	0.068		26.709	0.078		-30.820	
0.732	0.919	0.081		26.305	0.093		-30.356	
0.731	0.906	0.094	1.205	25.907	0.108	9.08E-01	-29.899	5.97E-11
0.731	0.894	0.106		25.516	0.123		-29.450	
0.730	0.881	0.119		25.131	0.137		-29.009	
0.730	0.869	0.131		24.753	0.151		-28.574	
0.729	0.857	0.143		24.380	0.165		-28.147	
0.729	0.845	0.155		24.014	0.179		-27.727	
0.728	0.834	0.166		23.654	0.192		-27.313	
0.728	0.822	0.178		23.300	0.205		-26.906	

Table A8. Experimental and calculated β_{ij} and P_i values

			β_{exp} [-]	β_{calc} [-]	P_i [mol/(m · s · Pa)]
X_m = 0,90	48 rpm	R1	1.205	1.183	5.97E-11
		R2	1.636	1.565	6.28E-11
		R3	2.138	2.003	5.89E-11
	40 rpm	R1	1.232	1.204	5.45E-11
		R2	2.595	2.425	4.27E-11
		R3	2.190	2.026	5.43E-11
	30 rpm	R1	1.566	1.478	5.18E-11
		R2	1.435	1.372	4.80E-11
		R3	2.041	1.874	5.09E-11
	20 rpm	R1	1.851	1.663	4.98E-11
		R2	2.838	2.528	3.65E-11
		R3	1.726	1.575	4.65E-11
X_m = 0,75	48 rpm	R1	15.149	13.092	7.71E-11
		R2	858993475.200	-5.765	8.65E-11
		R3	8.294	7.224	8.38E-11
	40 rpm	R1	66158207.754	-9.787	9.70E-11
		R2	13.975	11.642	8.15E-11
		R3	4.449	3.965	7.24E-11
	30 rpm	R1	4.545	3.942	6.93E-11
		R2	15.273	12.657	6.13E-11
		R3	4.878	4.099	7.77E-11
	20 rpm	R1	4.050	3.386	6.45E-11
		R2	5.409	4.487	5.70E-11
		R3	3.583	2.980	6.13E-11
X_m = 0,50	48 rpm	R1	50.703	40.098	1.57E-10
		R2	16.785	14.296	1.34E-10
		R3	10.238	9.324	1.07E-10
	40 rpm	R1	17.188	15.152	8.89E-11
		R2	3.743	3.406	1.14E-10
		R3	25.936	22.140	1.24E-10
	30 rpm	R1	4.411	3.835	9.41E-11
		R2	3.980	3.498	9.19E-11
		R3	4.574	3.983	9.85E-11
	20 rpm	R1	5.513	4.716	6.76E-11
		R2	21.202	17.884	6.21E-11
		R3	3.493	3.016	7.03E-11
X_m = 0,10	48 rpm	R1	2.177	2.126	4.24E-11
		R2	4.494	4.225	8.01E-11
		R3	6.596	6.048	1.00E-10
	40 rpm	R1	18.692	16.651	1.04E-10
		R2	9.824	8.743	1.06E-10
		R3	12.618	11.383	9.17E-11
	30 rpm	R1	16.635	14.434	9.74E-11
		R2	10.558	9.475	7.48E-11
		R3	12.765	10.926	1.06E-10
	20 rpm	R1	10.267	9.048	6.14E-11
		R2	71.949	59.785	8.57E-11
		R3	10.625	9.100	7.42E-11

Table A8. Experimental and calculated β_{ij} and P_i values (continued)

			β_{exp} [-]	β_{calc} [-]	P_i [mol/(m · s · Pa)]
X_m = 0,05	48 rpm	R1	13.810	11.715	2.12E-10
		R2	48.560	40.922	2.11E-10
		R3	7.113	6.518	1.19E-10
	40 rpm	R1	8.856	7.129	2.47E-10
		R2	27.433	22.279	2.22E-10
		R3	10.225	9.296	1.06E-10
	30 rpm	R1	28.619	25.017	1.08E-10
		R2	8.536	7.698	8.84E-11
		R3	7.971	7.076	1.03E-10
	20 rpm	R1	11.803	10.562	6.24E-11
		R2	536870922.000	-874.488	8.16E-11
		R3	65.325	53.951	1.03E-10
X_m = 0,01	48 rpm	R1	24.932	23.470	9.24E-11
		R2	901129924.200	-688.822	4.42E-10
		R3	16.911	11.449	6.06E-10
	40 rpm	R1	21.669	15.945	3.35E-10
		R2	17.746	11.928	4.36E-10
		R3	23.931	17.917	3.65E-10
	30 rpm	R1	34.786	24.573	2.95E-10
		R2	77.975	49.580	3.71E-10
		R3	202.309	108.685	5.62E-10
	20 rpm	R1	251.887	198.734	1.51E-10
		R2	224.808	180.190	1.48E-10
		R3	22.749	16.679	2.12E-10

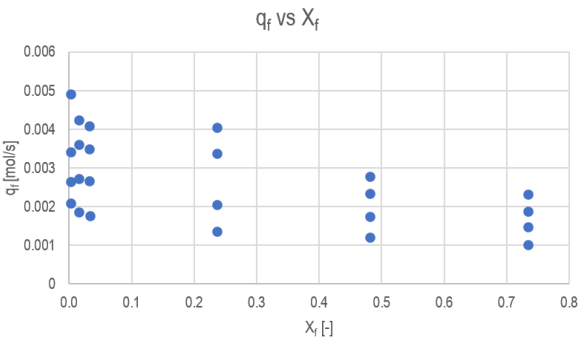

Figure A4. Feed flow (q_f) vs feed acetone molar fraction (X_f)

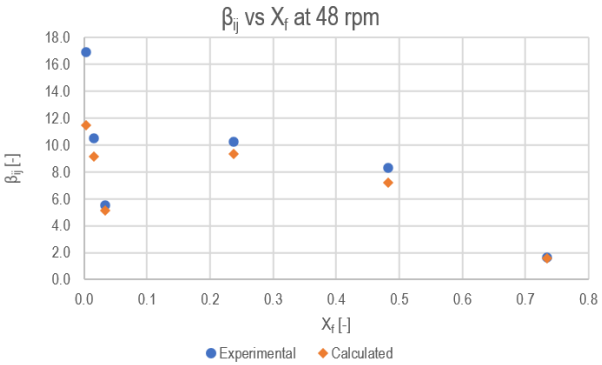

Figure A5. Separation factor (β_{ij}) vs feed acetone molar fraction (X_f) in the 48 rpm pump configuration

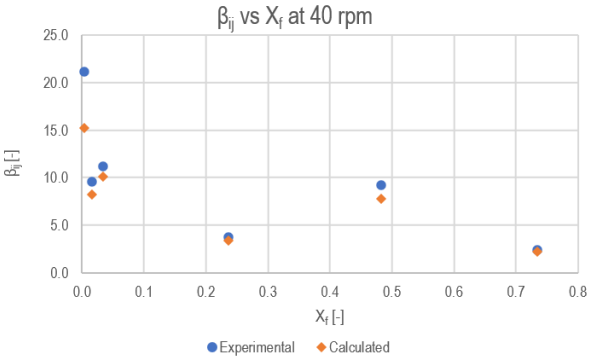

Figure A6. Separation factor (β_{ij}) vs feed acetone molar fraction (X_f) in the 40 rpm pump configuration

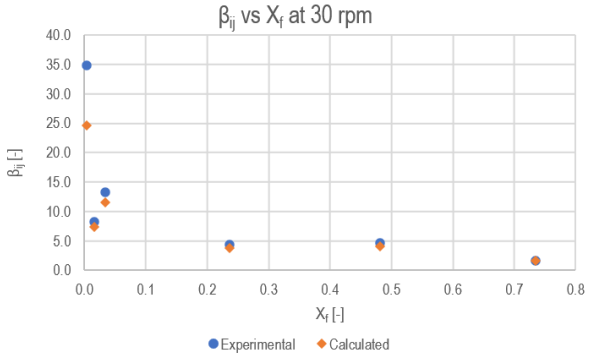

Figure A7. Separation factor (β_{ij}) vs feed acetone molar fraction (X_f) in the 30 rpm pump configuration

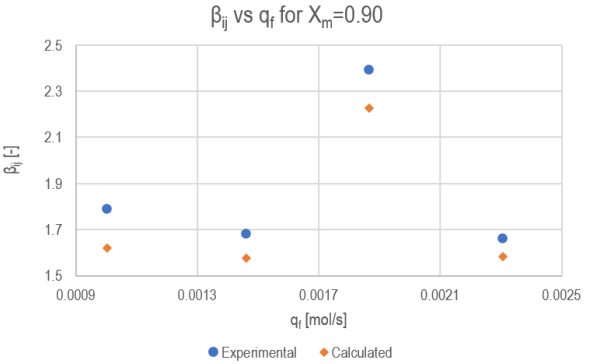

Figure A8. Separation factor (β_{ij}) vs feed flow (q_f) for X_m=0.90

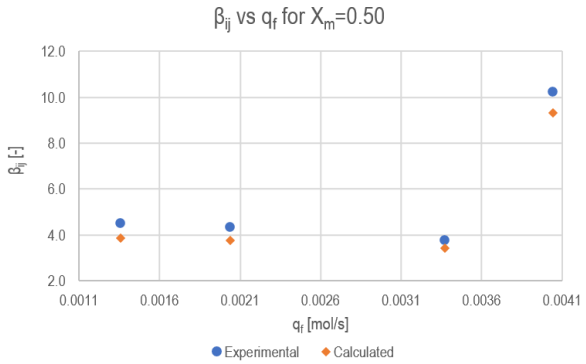

Figure A9. Separation factor (β_{ij}) vs feed flow (q_f) for X_m=0.50

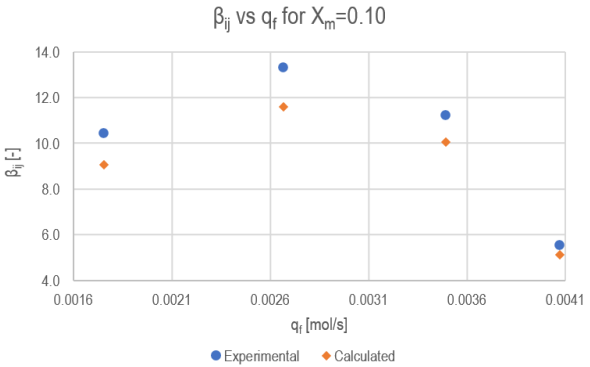

Figure A10. Separation factor (β_{ij}) vs feed flow (q_f) for X_m=0.10

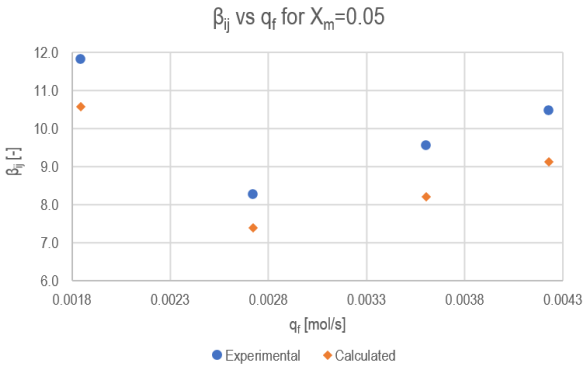

Figure A11. Separation factor (β_{ij}) vs feed flow (q_f) for X_m=0.05

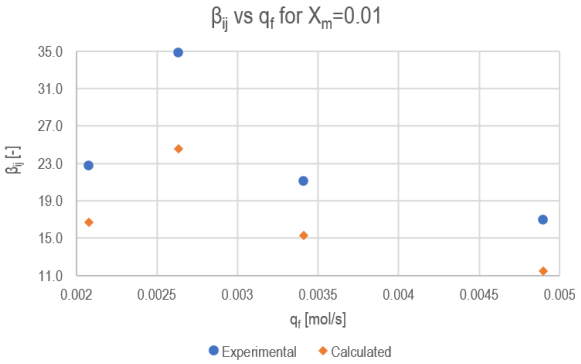

Figure A12. Separation factor (β_{ij}) vs feed flow (q_f) for X_m=0.01

APPENDIX 5: REPRESENTATIVE COMPOSITION OF THE ABE FERMENTATION PROCESS

Table A9. GC area percentage values of ABE feed and retentate mixture components

	GC area [%]			
	Water (peak 1)	Ethanol (peak 2)	Acetone (peak 3)	1-Butanol (peak 4)
ABE feed 1	0.988	9.943	30.958	58.111
ABE feed 2	1.080	10.024	30.885	58.011
ABE ret 1	0.968	10.669	17.730	70.634
ABE ret 2	0.841	10.710	17.649	70.800
ABE feed average	1.034	9.984	30.922	58.061
ABE ret average	0.905	10.690	17.690	70.717